TURUN YLIOPISTO
UNIVERSITY OF TURKU

Computationally Efficient AI in Brain-Tumour MRI and Physiological Signals in Sleep and Emotion Analysis

Dr. Muhammad Irfan

TURUN YLIOPISTON JULKAISUJA – ANNALES UNIVERSITATIS TURKUENSIS
SARJA – SER. F OSA – TOM. 84 | TECHNICA – INFORMATICA | TURKU 2026

TURUN YLIOPISTO
UNIVERSITY OF TURKU

COMPUTATIONALLY EFFICIENT AI IN BRAIN-TUMOUR MRI AND PHYSIOLOGICAL SIGNALS IN SLEEP AND EMOTION ANALYSIS

Dr. Muhammad Irfan

TURUN YLIOPISTON JULKAISUJA   ANNALES UNIVERSITATIS TURKUENSIS
SARJA   SER. F OSA   TOM. 84 | TECHNICA   INFORMATICA | TURKU 2026

University of Turku

Faculty of Technology
Department of Computing
Information and Communication Technology
Doctoral Programme in Technology

Supervised by

Prof. Tomi Westerlund
University of Turku, Finland

Prof. Wei Chen
University of Sydney, Australia

Reviewed by

Prof. David Grayden
University of Melbourne, Australia.

Prof. Huiru (Jane) Zheng
Ulster University, UK.

Opponent

Prof. Theodoros Arvanitis
University of Birmingham, UK

ISBN 978-952-02-0652-9 (PRINT)
ISBN 978-952-02-0653-6 (PDF)
ISSN 2736-9390 (Painettu/Print)
ISSN 2736-9684 (Sähköinen/Online)
Painosalama, Turku, Finland 2026

To my family and friends

UNIVERSITY OF TURKU
Faculty of Technology
Department of Computing
Information and Communication Technology
IRFAN, MUHAMMAD: Computationally Efficient AI in Brain-Tumour MRI and Physiological Signals in Sleep and Emotion Analysis
Doctoral dissertation, 111 pp.
Doctoral Programme in Technology
April 2026

ABSTRACT

In healthcare, diagnosing neurological and behavioural disorders depends on AI models that efficiently process complex data. However, many artificial intelligence (AI) models are too complex and resource-intensive, limiting their use in settings with limited computational power, battery capacity, or bandwidth. This thesis aims to develop AI that is both reliable and efficient in resource-limited environments, thereby maximising patient benefit. This thesis presents three contributions in medical imaging and signal analysis. First, it introduces two convolutional operators, Fuzzy Atrous Convolution (FAC) and Fuzzy Sigmoid Convolution (FSC), for binary brain-tumour classification from magnetic resonance imaging (MRI). Both methods improve feature extraction while reducing the number of parameters compared to standard CNNs. Despite their compactness, both models achieve state-of-the-art (SOTA) results. The FSC model achieves 0.9917, 0.9975, and 0.9989 in binary classification accuracy on three datasets, with 100 times fewer parameters than transfer-learning models. The FAC model achieves 0.9883, 0.9967, and 0.9956, outperforming SOTA models with 300 times fewer parameters, showing efficiency in inference time and size. Second, the thesis examines whether accurate neonatal sleep-stage classification can be achieved with reduced-channel EEG. Through multiview feature extraction, AdaptiSelect, and a data-reduction module, it reduces data transmission by 153.6 times while enabling full data reconstruction. On a four-year dataset, it achieves classification accuracy of 0.8116 ($Kappa = 0.7217$) with one EEG channel and 0.8279 ($Kappa = 0.7470$) with two channels under cross-validation. Leave-one-subject-out validation confirms its generalisability. It outperforms SOTA approaches in neonatal sleep analysis. Third, the thesis explores lightweight emotion-recognition models using single-modality electrocardiography. Accurate emotion detection is vital in human-computer interaction, mental health, and neurorehabilitation, where continuous, reliable evaluation improves outcomes. For edge monitoring, models must be computationally efficient. The approach employs multidomain feature extraction & fusion, and a voting model for low-power, real-time emotion tracking, ideal for wearables. The tailored model achieves an average accuracy of 0.9559 on the POPANE dataset, outperforming the general model's 0.6992. Comparisons show consistent improvement over past research.

KEYWORDS: Computational Efficiency, Medical Imaging, Physiological Signals, Brain Tumour MRI, Neonatal Sleep, Emotion Recognition, Lightweight AI

TURUN YLIOPISTO
Teknillinen tiedekunta
Tietotekniikan laitos
Tietotekniikka
IRFAN, MUHAMMAD: Computationally Efficient AI in Brain-Tumour MRI and Physiological Signals in Sleep and Emotion Analysis
Väitöskirja, 111 s.
Teknologian tohtoriohjelma
Huhtikuu 2026

TIIVISTELMÄ

Käytännön terveydenhuollossa neurologisten ja käyttäytymiseen liittyvien häiriöiden diagnosointi perustuu tekoälymalleihin, jotka kykenevät käsittelemään monimutkaista dataa tehokkaasti. Monet nykyiset tekoälymallit ovat kuitenkin liian monimutkaisia ja resurssi-intensiivisiä estäen niiden soveltamisen rajallisen laskentatehon, akkukapasiteetin tai tiedonsiirron kaistanleveyden yhteydessä. Tämän väitöskirjan tavoitteena on kehittää tekoälymenetelmiä, jotka ovat samanaikaisesti luotettavia ja resurssitehokkaita, jotta potilaiden saama hyöty voidaan maksimoida. Väitöskirjassa esitetään kolme tieteellistä kontribuutiota lääketieteellisen kuvantamisen ja signaalinkäsittelyn aloilta. Ensinnäkin esitellään kaksi uutta konvoluutio-operaattoria FAC ja FSC aivokasvainten luokitteluun magneettikuvantamisesta. Kompaktista rakenteestaan huolimatta molemmat mallit saavuttavat alan huipputason suorituskyvyn. FSC-malli saavuttaa tarkkuudet 0,9917, 0,9975 ja 0,9989 kolmessa eri aineistossa käyttäen sata kertaa vähemmän parametreja kuin siirtovaikutukseen perustuvat mallit. FAC-malli saavuttaa vastaavasti tarkkuudet 0,9883, 0,9967 ja 0,9956 ja päihittää alan huipputason verkot noin 300 kertaa pienemmällä parametrimäärällä, mikä osoittaa sen tehokkuuden sekä inferenssiajan että mallikoon suhteen. Toiseksi väitöskirjassa kehitetään resurssitehokas vastasyntyneiden univaiheiden luokittelujärjestelmä, joka hyödyntää yksi- ja kaksikanavaista elektroenkefalografiaa (EEG). Moninäkymäiseen piirteiden poimintaan, AdaptiSelect-menetelmään ja datanreduktiomoduuliin perustuva ratkaisu vähentää tiedonsiirtotarvetta153,6 kertaisesti mahdollistaen samalla alkuperäisen datan täydellisen rekonstruoinnin. Neljän vuoden aikana kerätyllä aineistolla järjestelmä saavuttaa ristiinvalidoinnissa yhden EEG-kanavan asetelmassa tarkkuuden 0,8116 ($\kappa = 0,7217$) ja kahden kanavan asetelmassa 0,8279 ($\kappa = 0,7470$). Kolmanneksi väitöskirjassa tarkastellaan kevyitä tunteentunnistusmalleja, jotka hyödyntävät yksimodaalista elektrokardiografiaa (ECG). Reaaliaikaista seurantaa varten mallien on oltava laskennallisesti kevyitä. Menetelmä soveltuu erityisen hyvin puettaville laitteille. Räätälöity malli saavuttaa POPANE-aineistolla tarkkuuden 0,9559, mikä ylittää selvästi yleistetyn mallin tarkkuuden 0,6992. Vertailut aiempaan tutkimukseen osoittavat suorituskyvyn parantuneen johdonmukaisesti.

Avainsanat: laskennallinen tehokkuus; lääketieteellinen kuvantaminen; fysiologiset signaalit; aivokasvaimen magneettikuvaus (MRI); vastasyntyneiden uni; tunteentunnistus; kevyet tekoälymallit.

Acknowledgements

I extend my deepest gratitude to my supervisor, Professor Tomi Westerlund, and to Professor Wei Chen, whose guidance and encouragement have been invaluable throughout this journey. I am profoundly grateful to my parents, my brothers, and my sister. Your unwavering love has been my anchor. To my wife (Fatima Batool) and children (Emaan Fatima and Muhammad Mikail Irfan), thank you for your patience, support, and constant inspiration. I am also thankful to my friends who walked alongside me, whether near or far, offering encouragement when it was needed most. Above all, I am grateful to Allah for granting me the strength and perseverance to complete this PhD journey. This milestone is not mine alone; it belongs to all of us.

Date: 2025.11.18
Dr. Muhammad Irfan

DR. MUHAMMAD IRFAN
I am a senior researcher and principal investigator working in artificial intelligence for healthcare, with a focus on AI-enabled health monitoring, treatment support, and translational medical imaging. My research spans multimodal biomedical signal and image analysis (MRI, CT, PET), edge and federated learning, and generative AI, with applications in brain and head-and-neck cancers, stroke, and dementia care. I hold a PhD in biomedical engineering from Fudan University and am completing a second PhD at the University of Turku. I have published articles in leading IEEE transactions and journals, as well as in Elsevier journals, and have secured competitive national and international research funding.

Table of Contents

Abbreviations

AI	Artificial Intelligence
ML	Machine Learning
SOTA	State-of-the-Art
MRI	Magnetic Resonance Imaging
CT	Computed Tomography
PET	Positron Emission Tomography
EEG	Electroencephalogram
EOG	Electrooculogram
EMG	Electromyogram
ECG	Electrocardiogram
PSG	Polysomnography
NICU	Neonatal Intensive Care Unit
CHFDU	Children's Hospital of Fudan University
W_S	Wake State
N_I	Stage N1 Sleep
N_{II}	Stage N2 Sleep
N_{III}	Stage N3 Sleep
A_S	Active Sleep
Q_S	Quiet Sleep
DTCWT	Dual-Tree Complex Wavelet Transform
FAWT	Flexible Analytic Wavelet Transform
ECOV	Eigenvector Covariance Features
MSPCA	Multiscale Principal Component Analysis
STREAM	Smart Cloud Data Transfer and Reconstruction Module
FS	Feature Selection
KBest	SelectKBest Univariate Feature Selection
CNN	Convolutional Neural Network
HNN	Hierarchical Neural Network
MS-HNN	Multi-Scale Hierarchical Neural Network
MBCNN	Multi-Branch Convolutional Neural Network
BiLSTM	Bidirectional Long Short-Term Memory Network
LR	Logistic Regression
GNB	Gaussian Naive Bayes

SVM	Support Vector Machine
DT	Decision Tree
RF	Random Forest
XTRA	ExtraTrees Classifier
KNN	k-Nearest Neighbours
MLP	Multilayer Perceptron
HMM	Hidden Markov Model
CV	Cross-Validation
LOSO-CV	Leave-One-Subject-Out Cross-Validation
Acc.	Accuracy
Pre.	Precision
Rec.	Recall
F1	F1-Score
Kappa	Cohen's Kappa Coefficient
MCC	Matthews Correlation Coefficient
AUC	Area Under the ROC Curve

List of Original Publications

This dissertation is based on the following original publications, which are referred to in the text by their Roman numerals:

I Irfan, M., Subasi, A., Mehdi, H., Westerlund, T. and Chen, W., 2024, December. Fuzzy-Based Atrous Convolution for Brain Tumor Detection Using MRI. In 2024 IEEE International Conference on Progress in Informatics and Computing (PIC) (pp. 280-289). doi: 10.1109/PIC62406.2024.10892686.

II Irfan, M., A. Nawaz, R. Klén, A. Subasi, T. Westerlund and W. Chen, "Improved Brain Tumor Detection in MRI: Fuzzy Sigmoid Convolution in Deep Learning," 2025 International Joint Conference on Neural Networks (IJCNN), Rome, Italy, 2025, pp. 1-8,
doi: 10.1109/IJCNN64981.2025.11227858.

III Irfan, M., Wang, L., Xu, Y., Subasi, A., Chen, C., Klen, R., Westurlund, T. and Chen, W., 2025. Smart iot-based solutions for neonatal sleep stratification: Single-dual channel eeg, adaptiselect, multview fusion, & rotational ensemble stacking. IEEE Internet of Things Journal.
doi: 10.1109/JIOT.2025.3558235

IV Irfan, M., Nawaz, A., Bulbul, A.K., Klén, R., Subasi, A., Westerlund, T. and Chen, W., 2025. Emotion recognition with minimal wearable sensing: Multi-domain feature, hybrid feature selection, and personalized vs. generalized ensemble model analysis. In: Proceedings of the 2025 IEEE International Conference on Bioinformatics and Biomedicine (BIBM), pp. 5447–5453. https://doi.org/10.1109/BIBM66473.2025.11356135

V Bulbul, A.K., Irfan, M., Jaakkola, M.K., Subasi, A. and Klén, R., 2025. Wearable-based Emotion Recognition Using Electrocardiogram and Galvanic Skin Response and Instrumentation Audit: A Systematic Review. IEEE Transactions on Instrumentation and Measurement, under review.

Publications not included in Thesis

The following publications are thematically related to the work presented in this thesis, but are not included as part of the compiled dissertation. They either address adjacent methodological developments, earlier investigations, or parallel research contributions conducted during the doctoral period.

II Irfan, M., Shun, P., Felix, B.B., Mustafa, N., Abbasi, S.F., Nahli, A., Subasi, A., Westerlund, T. and Chen, W., 2023. An IoT-based noncontact ECG system: sole of the feet/hands palm. IEEE Internet of Things Journal, 10(21), pp.18718-18732.

I Nawaz, A., Irfan, M., Yu, X., Zou, Z. and Westerlund, T., 2025. "Blockchain-Enabled Privacy-Preserving Second-Order Federated Edge Learning in Personalised Healthcare," in IEEE Transactions on Consumer Electronics, doi: 10.1109/TCE.2025.3620115.

III Nawaz, A., Wang, L., Irfan, M. and Westerlund, T., 2024. Hyperledger Sawtooth-based supply chain traceability system for counterfeit drugs. Computers & Industrial Engineering, 190, p.110021.

IV Siddiqa, H.A., Tang, Z., Xu, Y., Wang, L., Irfan, M., Abbasi, S.F., Nawaz, A., Chen, C. and Chen, W., 2024. Single-Channel EEG data analysis using a multi-branch CNN for neonatal sleep staging. IEEE Access, 12, pp.29910-29925.

V Irfan, M., Subasi, A., Mustafa, N., Westerlund, T. and Chen, W., 2024. An evaluation of pretrained convolutional neural networks for stroke classification from brain CT images. In Applications of Artificial Intelligence in Healthcare and Biomedicine (pp. 111-135). Academic Press.

VI Nawaz, A., Irfan, M., Sadiqa, H.A. and Westerlund, T., 2023, November. Edge-based skin cancer decision support system using machine learning algorithms. In 2023 IEEE Intl Conf on Dependable, Autonomic and Secure Computing, Intl Conf on Pervasive Intelligence and Computing, Intl Conf on Cloud and Big Data Computing, Intl Conf on Cyber Science and Technology Congress (DASC/PiCom/CBDCom/CyberSciTech) (pp. 0292-0297). IEEE.

VII Ferreira, A., *et al.* (incl. Irfan, M.) (2025). AI and co-design to support dementia: lessons from a first co-creation session. In *Proc. International Conference on Computer-Human Interaction Research and Applications (CHIRA 2025)*, pp. 1–1. Available: https://chira.scitevents.org/Home.aspx?y=2025 (Accepted but yet to be published at Springer)

VIII Irfan, M., Subasi, A., Tang, Z., Wang, L., Xu, Y., Chen, C., Westurlund, T. and Chen, W., 2025. A novel nicu sleep state stratification: Multiperspective features, adaptive feature selection and ensemble model. IEEE Transactions on Biomedical Engineering.

IX Irfan, M., Wang, L., Shahid, H., Xu, Y., Subasi, A., Munawar, A., Mustafa, N., Chen, C., Westurlund, T. and Chen, W., 2025. Multidomain selective feature fusion and stacking-based ensemble framework for EEG-based neonatal sleep stratification. IEEE Journal of Biomedical and Health Informatics.

X Irfan, M., Jawad, H., Felix, B.B., Abbasi, S.F., Nawaz, A., Akbarzadeh, S., Awais, M., Chen, L., Westerlund, T. and Chen, W., 2021. Non-wearable IoT-based smart ambient behaviour observation system. IEEE Sensors Journal, 21(18), pp.20857-20869.

XI Nawaz, A., Irfan, M. and Westerlund, T., 2023, September. Optical character recognition using optimised convolutional networks. In 2023 Eighth International Conference on Fog and Mobile Edge Computing (FMEC) (pp. 107-114). IEEE.

XII Sharma, N., Hwang, Y., Irfan, M., Subasi, A. (2025). Lung cancer detection from histopathological imaging using knowledge graphs and graph neural networks. In: Generative AI, Large Language Models, Graph Neural Networks and Knowledge Graphs: Applications. Book chapter, accepted for publication (forthcoming).

1 Introduction

Artificial intelligence (AI) has made significant improvements in neurological and behavioural health, including cancer triage in neuroimaging, assessing sleep in newborns, and monitoring affective states. Yet, environments where prompt decisions are crucial, such as busy clinics, neonatal intensive care units (NICUs), and home settings, function with severely limited resources: limited on-site computing power, restricted battery life, and narrow or unreliable network connections. In such scenarios, it's challenging to utilise today's large-scale multimodal models consistently and effectively. Modern deep neural networks can achieve good accuracy but are often too large for resource-constrained clinical and wearable settings. This challenge led to the development of parameter-efficient Convolutional Neural Networks (CNNs) families (including SqueezeNet, MobileNetV2, and EfficientNet) that maintain accuracy while using significantly fewer parameters [1; 2; 3]; however, their deployment remains very limited. In neuro-oncology, deep learning has become a common approach for Magnetic Resonance Imaging (MRI) classification and segmentation. Recent reviews summarise both the promise and the deployment limitations, highlighting the necessity for lightweight, clinically integrable models. [4; 5; 6]. This thesis explores computationally efficient methodologies that maintain diagnostic effectiveness while minimising parameters, possibilities that can reduce energy consumption, and transmission requirements, thereby enhancing accessibility to AI-driven healthcare.

1.1 Brain-Tumour

The human brain serves as the central hub for vital functions such as memory, speech, cognition, and motor skills [7; 8; 9]. Any irregular or uncontrolled growth of brain tissue can disrupt these functions, leading to the development of brain tumours [10]. Because these tumours vary widely in type, behaviour, and severity, they present substantial challenges for both patients and healthcare providers.

1.1.1 Brain Tumour Assessment Modalities

The assessment and characterisation of brain tumours typically involve a combination of complementary imaging modalities, primarily MRI, computed tomography

(CT), and positron emission tomography (PET), in conjunction with advanced MRI techniques such as diffusion, perfusion, and spectroscopy, and, when accessible, hybrid (PET and MRI). Fig 1 shows images of PET, CT, and MRI, respectively. MRI provides detailed images of the brain and other tissues; CT scans quickly identify and show bleeding, calcification, and bone; and PET scans provide information on metabolism and function. These methods work together to aid in diagnosis, plan surgery and radiation therapy, monitor treatment effectiveness, and track patients over time.

MRI: It is the primary modality in neuro-oncology due to its exceptional soft-tissue contrast and comprehensive multiparametric readouts. Standard T1-, T2-, and FLAIR sequences (with or without gadolinium) demonstrate differences between enhancing tumours, non-enhancing infiltrative components, vasogenic oedema, and mass effect. Diffusion-weighted imaging (DWI) with apparent diffusion coefficient (ADC) maps approximates cellularity; dynamic susceptibility contrast and dynamic contrast-enhanced perfusion, and arterial spin labelling where available, quantify haemodynamics, such as relative cerebral blood volume, permeability that correlate with grade; and proton MR spectroscopy yields a metabolic profile (elevated choline, reduced N-acetylaspartate, and lipid-lactate peaks) that helps distinguish tumour from treatment effect or radiation necrosis. MRI accomplishes this without ionising radiation, facilitating secure serial follow-up along the disease trajectory [11].

CT: It remains important when rapid imaging is required or when MRI is contraindicated. CT is particularly useful for detecting acute intracranial haemorrhage, visualising calcifications suggestive of oligodendroglioma, assessing osseous involvement, and quantifying mass effect in emergency settings. Although CT lacks MRI's soft-tissue contrast, its rapid acquisition and wide availability make it the typical first-line study in urgent presentations and a useful adjunct for specific tumour features [11].

PET: It contributes functional and metabolic context beyond morphology. Amino-acid tracers such as ^{18}F-FET, ^{18}F-FDOPA, and ^{11}C-methionine exploit upregulated amino-acid transport in gliomas, yielding high tumour-to-background contrast that supports precise delineation, biopsy targeting, radiotherapy planning, and differentiation of recurrence from treatment-related change. By contrast, ^{18}F-FDG is less specific for primary brain tumours because of high cortical glucose uptake. In combination with MRI, amino-acid PET refines diagnosis and guides management throughout the tumour lifecycle [12].

CT and PET offer additional structural and metabolic data, respectiveprovide additional structural and metabolic data, respectively; however, MRI remains treatment planning, and longitudinal monitoring of brain tumours, ensuring a balance between diagnostic accuracy and safety for repeated imaging.

(a) (b) (c)

Figure 1. Representative neuro-imaging modalities for brain-tumour assessment: (a) PET; (b) CT; (c) MRI [13]

1.1.2 Architecture Efficiency in Brain-Tumour MRI

Deep learning methods have been extensively explored for brain tumour detection using MRI data in recent years [14; 15; 16]. Several studies have applied various deep learning models, achieving different levels of accuracy and offering diverse findings in brain tumour diagnosis [17; 18]. Most studies have utilised CNNs to improve the precision of brain tumour classification, ranging from binary to multistage classification [19; 16]. Furthermore, recent studies demonstrate the various methods and models available for brain tumour classification and segmentation. However, while high-performing models, such as Resnet50 and EfficientNet, achieve high precision [19; 20; 21; 22], these performance gains often come at the cost of substantially increased model complexity. Large transfer-learning architectures such as ResNet50 and EfficientNetB0 contain millions of trainable parameters, which increase memory use, computational cost, and inference burden. To address this issue, we propose two approaches, FAC and FSC, along with two modules: top of the funnel (TOFU) and middle of the funnel (MOFU), designed to provide highly accurate predictions with significantly fewer parameters. Both approaches have their advantages and limitations in terms of performance and computational requirements.

In **Publication I**, a Fuzzy Atrous Convolution (FAC) architecture with two additional modules, TOFU and MOFU, has been proposed for binary brain-tumour classification from MRI with the aim of developing a computationally efficient model with fewer trainable parameters while maintaining high classification accuracy. A novel convolutional operator is introduced in the FAC model to enlarge the receptive field while preserving input information, thereby enabling efficient feature-map reduction and accurate tumour detection. Compared with large transfer-learning models, the proposed method uses approximately 300 times fewer trainable parameters, making it particularly suitable for efficient early classification of brain tumors.

In **Publication II**, a fuzzy sigmoid convolution (FSC) layer is introduced to develop a lightweight and computationally efficient model that reduces the number of trainable parameters without compromising classification accuracy. The proposed methodology significantly reduces the number of trainable parameters without compromising classification accuracy. A novel convolutional operator is central to this approach, as it employs dilated convolutions to enlarge the effective receptive field. Meanwhile, fuzzy sigmoid-based membership functions adaptively reweight high- and low-activation responses, rather than discarding them. This design enables computationally efficient feature representation and enhances the model's tumour detection capability. In the FSC-based model, fuzzy sigmoid activations are directly integrated into the convolutional layers to enhance feature extraction and classification. The incorporation of fuzzy logic enhances the network's adaptability and robustness to input variability. Extensive experiments on three benchmark brain tumour MRI datasets demonstrate the performance and efficiency of the proposed model. The model employs approximately 100 times fewer trainable parameters than large-scale transfer-learning architectures, highlighting its computational efficiency and suitability for early detection of brain tumours. This research presents lightweight, high-performance deep learning models for brain tumour stratification.

1.2 Wearable technology

Simple and unobtrusive wearables, particularly watches and wristbands, now enable continuous monitoring with minimal inconvenience and are now mainstream, with 534.6M units shipped in 2024, and older adults are already using them (38 % of U.S. 50+ own a wearable; 71 % use health/wellness apps), making them a practical foundation for emotion-aware care, as reported by IDC [23; 24]. Fig. 2 from (**Publication V**) illustrates the general wearable device system, which includes the collection of physiological signals from body sensors, cloud-based data transmission, and alerts sent to family, emergency services, and healthcare providers.

1.2.1 Neonatal Sleep Analysis

In 2020, the situation became increasingly dire, with newborn mortality escalating to a concerning high of 2.4 million deaths during the first month. This corresponds to over 6,700 daily fatalities, accounting for 47 % of all child deaths under five, a significant rise from 40 % in 1990 [25; 26]. While these figures are not specifically about sleep disorders, they emphasise the necessity of enhanced monitoring for newborns and the need for early intervention.

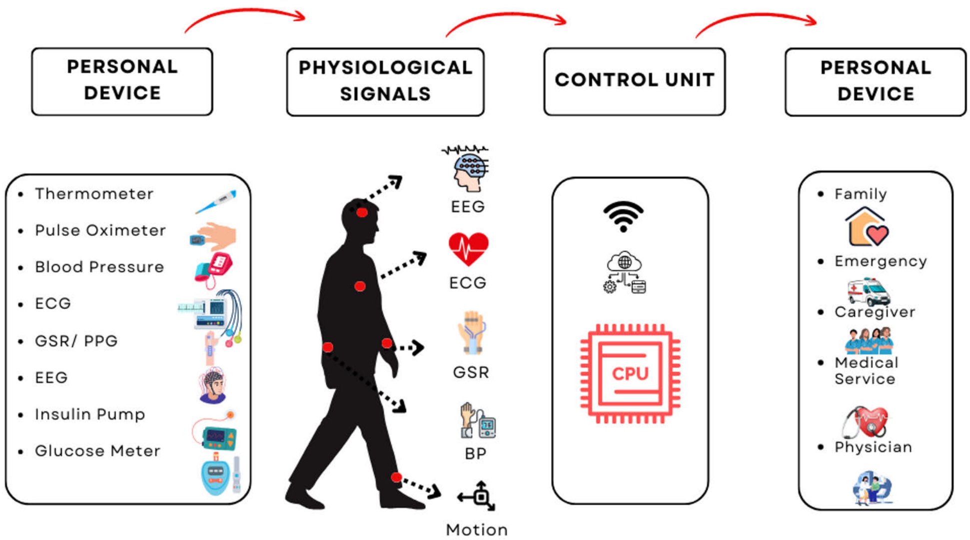

Figure 2. General diagram for wearable devices.

Sleep Assessment Modalities

A range of physiological monitoring modalities are used to help healthcare professionals and researchers assess sleep patterns and cardiac function. These modalities are particularly important for evaluating sleep-related disorders and cardiovascular health in diverse populations, from neonates to older adults. Key methods include electroencephalography (EEG), electrocardiography (ECG), electrooculography (EOG), electromyography (EMG), photoplethysmography (PPG), as well as audio and video recordings. Each modality provides distinct insights into underlying physiological processes, supporting the diagnosis and management of various health conditions.

ECG: ECG is the gold standard for monitoring the heart's electrical activity, especially useful for assessing heart rate variability (HRV), arrhythmias, and sleep-related cardiovascular issues, such as sleep apnea. It directly measures the heart's electrical conduction, providing high accuracy for detecting even the most subtle arrhythmias. It also provides real-time insights into the autonomic regulation of the heart during sleep, which is crucial for understanding heart health.

EEG: EEG is a core modality for assessing brain function during sleep, offering real-time, high-temporal-resolution measurements of neural electrical activity. By capturing subtle and complex brainwave dynamics, EEG enables the identification of sleep disorders and functional abnormalities that are often difficult to detect using other assessment techniques.

Importance of EEG for Sleep Analysis: Although auxiliary signals such as EMG and EOG provide complementary information, EEG remains the primary modality for identifying and classifying sleep stages because it directly measures neural activity. Many sleep disorders, including sleep apnea, insomnia, and parasomnias, are associated with alterations in brain dynamics that are most reliably captured through EEG recordings. EEG is particularly important in neonatal sleep research, where developmental changes in brainwave patterns are closely linked to neurodevelopmental outcomes. In this thesis, a reduced number of EEG channels is employed to improve efficiency and practicality. Multimodal approaches that combine EEG with additional physiological sensors such as EMG or EOG are intentionally excluded. The goal is to simplify data acquisition while preserving diagnostic accuracy and robustness. Reducing channel count enables less intrusive monitoring, lowers computational and hardware requirements, and remains effective through the use of optimised machine learning models.

EOG: EOG assesses eye movements and is essential for detecting rapid eye movement (REM) sleep, characterised by distinctive eye activity. The EOG records electrical potentials produced by eye movements, facilitating the distinction between sleep stages, especially REM and non-REM phases. Nonetheless, EOG does not directly measure cerebral activity, thereby offering less comprehensive insights into the underlying neurological processes compared to EEG. Consequently, EOG is frequently utilised in conjunction with EEG to facilitate a more thorough examination of sleep.

EMG: EMG measures the activity of muscles and is valuable for evaluating muscle tone and movement during sleep. It is crucial for diagnosing motion-related sleep disorders, including REM sleep behaviour disorder and periodic limb movement disorder, which are marked by irregular or excessive muscle activation. In sleep research, EMG is generally utilised as an additional signal to EEG rather than as the principal modality for sleep staging.

PPG: PPG quantifies variations in blood volume in peripheral microvascular tissue by optical sensing, facilitating non-invasive assessment of heart rate and oxygen saturation during sleep. While PPG is easy and extensively utilised in wearable devices, it offers inferior temporal precision and signal integrity compared to electrocardiography (ECG) for comprehensive cardiovascular evaluation. As a result, PPG is predominantly utilised for general wellness monitoring rather than for clinical-grade heart assessment in sleep research.

Audio and Video Data: Audio and video recordings have been utilised in sleep research to record snoring, bodily movements, and other observable behaviours linked to sleep problems. Nonetheless, video-based monitoring is computationally intensive and often yields imprecise results, such as binary classifications of sleep versus wakefulness, with limited physiological interpretability. In contrast to biosignals like EEG or ECG, audio-visual data provide diminished granularity for multi-stage sleep monitoring. Furthermore, ongoing recording presents significant privacy and ethical concerns, especially in neonatal environments. This study excludes audio- and video-based methodologies for these reasons. The emphasis is on improving EEG analysis to attain precise, multi-stage sleep classification while minimising computational complexity.

1.2.2 EEG

EEG is a non-invasive electrophysiological method commonly utilised to capture brain activity from the cerebral cortex. Due to its improved temporal resolution, EEG is exceptionally useful in studying fast brain dynamics and transitory neurological processes in real time. The central nervous system principally consists of neurones and glial cells [27]. Neurones provide information transfer via electrical and chemical signalling, whereas glial cells offer crucial structural, metabolic, and functional support. Despite not generating action potentials, glial cells are essential for preserving synaptic integrity, controlling the extracellular milieu, and facilitating neuronal signaling [28]. Neural communication transpires at synapses, where the arrival of an action potential at the presynaptic terminal triggers the release of neurotransmitters into the synaptic cleft. These neurotransmitters bind to specific receptors on the postsynaptic membrane, leading to the opening and closing of ion channels that generate postsynaptic potentials. EEG signals are obtained by placing electrodes on the scalp to record aggregate electrical activity primarily generated by synchronised postsynaptic potentials from extensive neuronal populations [29].

EEG recordings do not capture single neuronal spikes; instead, they reflect the aggregate of excitatory and inhibitory currents across broad cortical areas. The amplitude of the recorded signal is significantly influenced by the level of temporal synchronisation among neurones: coherent activity increases signal amplitude, while asynchronous activity leads to signal attenuation. Factors affecting EEG voltage encompass the spatial distribution, orientation, and intensity of underlying current sources. Cortical pyramidal neurones are the primary contributors to EEG signals owing to their prevalence, parallel orientation, and extensive dendritic architecture. The structured arrangement of these neurones promotes the aggregation of ionic currents, producing extracellular electric fields that can be detected at the scalp surface. Thus, the activity of pyramidal cells has a significant influence on the EEG signal recorded during sleep and various cognitive states.

EEG Recording Clinical EEG systems comprise numerous critical components, including scalp electrodes (which are frequently silver/silver chloride), lead cables, signal amplifiers, and a computer unit responsible for system control, data storage, and visualisation. The EEG acquisition pipeline is depicted in a simplified manner in Fig. 3. Electrodes serve as the interface between neural electrical activity and the recording apparatus, measuring voltage differentials at specified scalp locations. Electrodes are often classified into two types: invasive needle electrodes, which pierce the subdermal tissue, and non-invasive disc electrodes, which are placed on the scalp surface.

In neonatal clinical practice, sleep monitoring typically commences shortly after birth, especially for newborns considered at increased risk of neurological or sleep-related problems. Ongoing or recurrent observation throughout this first developmental phase provides significant insight into cerebral maturation and functional organisation during sleep. Examining newborn sleep architecture is essential for detecting unusual patterns that may indicate underlying neurological or developmental disorders [30]. Electrode placement is generally conducted by qualified clinical personnel following established protocols [31].

Neonatal EEG recordings often utilise the worldwide 10–20 method for electrode placement, which is based on defined cranial landmarks to guarantee reproducibility and anatomical significance. Based on clinical aims and practical limitations, either the complete montage or a smaller selection of electrodes may be utilized [32]. In reduced-channel setups, electrodes are commonly situated over the biparietal areas (P3 and P4). Recent methodologies have extended limited montages to include central (C3, C4) and frontal (F3, F4) sites, thus enhancing sensitivity to sleep-associated cortical activity while ensuring practicality in newborn environments [33].

In standard clinical EEG recordings, a referential montage is often employed. In this setup, one electrode serves as the reference point, and the EEG system measures the voltage differences between this reference and all other electrodes [34]. For the review and analysis of neonatal EEG data, a bipolar montage is frequently used, where the voltage difference is calculated between pairs of electrodes, often adjacent ones. This method is particularly advantageous for artefact reduction, providing clearer and more accurate data for clinical interpretation [34].

EEG as a Neonatal Sleep Modality

In 1924, Hans Berger reported the first human electroencephalography (EEG) recordings, thereby establishing non-invasive testing of brain function. Loomis and colleagues introduced EEG-based sleep pattern analysis in 1937, marking one of the first systematic applications of EEG in human sleep research [35; 36; 35].

In modern NICUs, EEG is a common technique for neurological assessment, evaluation of brain maturation, and detection of abnormalities [37]. The standard re-

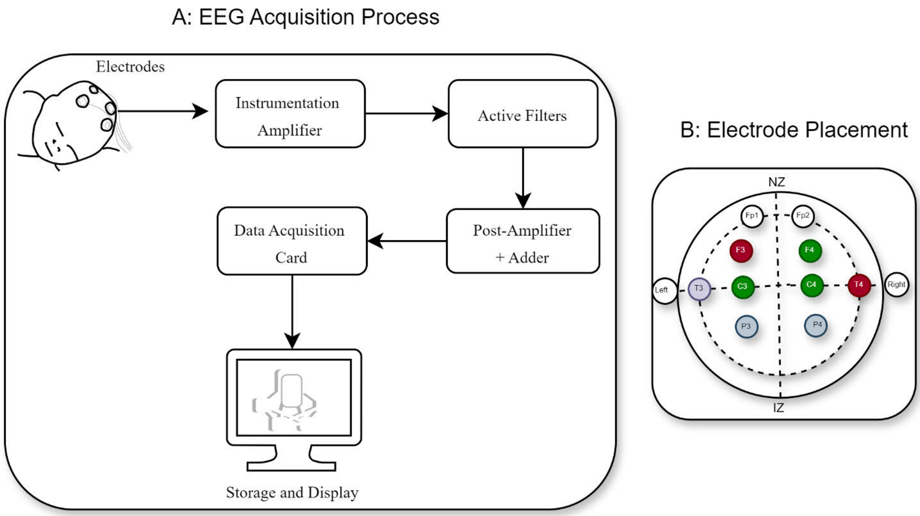

Figure 3. A) Schematic overview of the EEG acquisition system. B) Electrode layout based on the neonatal-adapted international 10–20 system, with the five channels identified as most informative in this thesis highlighted in red and green.

mains the clinical reference for monitoring brain function, detecting sleep disorders, and diagnosing newborn encephalopathy [38; 32; 39; 40; 41; 32; 42]. Depending on the clinical question, EEG recordings may be brief “snapshot” studies lasting several minutes to a few hours or prolonged recordings lasting many hours to days, often as part of a polysomnography (PSG) protocol for detailed analysis of sleep architecture.

PSG: PSG is the standard for assessing sleep disorders and behaviour since its introduction in the 1960s ([43]). PSG uses a polygraph, a piece of equipment that captures numerous physiological signals nightly in a sleep lab. The EEG, ECG, pulse rate, and EMG signals obtained during PSG are shown in Fig. 4.

Sleep Disorders Assessed with PSG: PSG plays a central role in diagnosing several major sleep disorders:

- **Sleep Apnea:** Recurrent upper-airway obstruction causes apneas, hypopneas, and fragmented sleep. PSG detects these events, snoring, and associated changes in oxygen saturation, heart rate, and respiratory effort, enabling severity grading.

- **Insomnia:** Defined by difficulty initiating or maintaining sleep, PSG helps identify prolonged sleep latency, reduced sleep efficiency, and altered REM architecture, supporting the diagnosis and management of chronic insomnia.

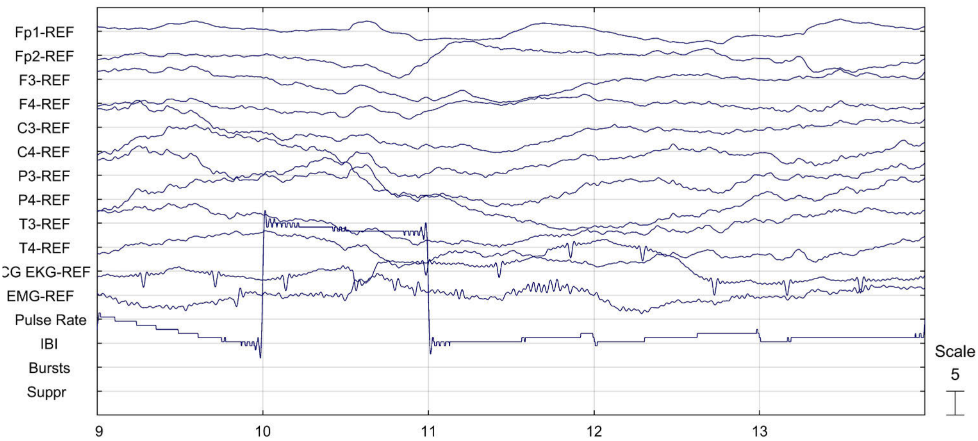

Figure 4. An Overview of EEG, ECG, and EMG Signals Collected via PSG Using a Multichannel Approach

- **Periodic Leg Movements Disorder:** Involves stereotyped, repetitive leg movements during sleep. PSG quantifies these movements and their associated arousals, clarifying their impact on sleep continuity and quality.

1.2.3 Common Neonatal EEG Artefacts

Neonatal EEG recordings are highly susceptible to artefacts from both physiological sources, such as movement, ECG, muscle activity, sweat and non-physiological sources such as electrode problems, electrical interference, which can obscure true cerebral activity and complicate interpretation [44; 45; 46; 47; 48; 49]. Recognising these artefacts and understanding their typical appearance is essential for reliable clinical use and for the development of automated analysis methods.

Movement artefacts are typically caused by limb or head motion and can produce high-amplitude transients that overshadow the underlying EEG signal. ECG artefacts appear as regular, periodic deflections that are particularly prominent when brain activity is suppressed. Muscle activity generates small-amplitude, high-frequency, stochastic noise superimposed on the EEG. Electrical interference from equipment and power lines produces spurious spikes or rhythmic oscillations. Electrode-related artefacts arise from poor contact or electrode movement and manifest as abrupt, often high-frequency disturbances, while sweat artefacts alter scalp conductivity and frequently introduce slow-wave components [44; 45; 46; 47; 48; 49]. Mitigation strategies include careful infant positioning, maintaining a calm environment, proper skin preparation and electrode placement, regular impedance checks, appropriate filtering, and minimising environmental electrical noise.

Artefacts present a major obstacle for automated background classification in neonatal EEG, especially in infants with pathological backgrounds, because they can both mimic and mask clinically relevant patterns [45; 46; 47; 49; 50; 51]. Most existing artefact-handling methods are designed for specific artefact types and do not generalise well to the heterogeneous and dynamic artefacts encountered in long-term neonatal monitoring, which can degrade system performance [52; 53]. A recent study by Webb et al. [49] proposed a deep-learning-based approach to classify EEG segments as artefact-free or artefact-contaminated, highlighting a promising direction toward more robust, artefact-aware neonatal EEG analysis.

1.2.4 Validation and Comparison to the Gold Standard

A critical step in developing any automated tool for clinical practice involves thorough validation and comparison to the gold standard. In the context of neonatal sleep monitoring, the gold standard typically refers to expert annotations or scores derived from the visual interpretation of EEG data, as discussed in Section 1.2.5. Visual interpretation represents the upper limit of classifier performance, as it captures the inherent variability in human annotations, setting the benchmark against which automated classifiers are evaluated.

1.2.5 Visual EEG Interpretation and Inter-Rater Agreement

Visual interpretation of neonatal EEG by expert clinicians remains the clinical gold standard but is inherently subjective, as complex and imperfect scoring systems do not fully account for medication effects, pathological conditions, or artefacts, leading to substantial intra- and inter-rater variability [54; 55; 56]. To quantify consistency between reviewers, inter-rater agreement is commonly assessed using Cohen's Kappa coefficient (κ), which measures agreement beyond chance [57]:

$$\kappa = \frac{P_o - P_e}{1 - P_e}, \tag{1}$$

where P_o is the observed agreement and P_e is the expected agreement by chance, given by

$$P_e = \frac{1}{N^2} \sum_k n_{k1} n_{k2}. \tag{2}$$

Kappa values range from -1 (less agreement than expected by chance) to $+1$ (perfect agreement), but are sensitive to class prevalence and sample composition, which can complicate their interpretation in EEG studies [58].

Clinically Significant EEG Characteristics

EEG Pattern Analysis: The EEG activity in newborns is characterised by several essential features, including amplitude, frequency, spatial distribution, and temporal evolution [59]. In preterm newborns, the EEG predominantly exhibits high-amplitude delta activity (below 4 Hz) alongside some theta activity (4–8 Hz), whereas term infants demonstrate heightened theta and alpha activity (8–12 Hz) as brain maturation occurs [60]. EEG patterns evolve with development, and characteristics such as continuity, reactivity, symmetry, synchronisation, and sleep-wake cycling (SWC) are critical indications of brain maturation. EEG continuity signifies a consistent amplitude, indicating more sophisticated neurological maturation, whereas discontinuity characterized by fluctuating high and low-amplitude bursts, generally suggests an immature, developing brain. The reactivity of the EEG is manifested as signal modulation in reaction to external stimuli, providing insights into the brain's functioning status [61].

The emergence of SWC, which becomes distinctly recognisable at 30 weeks postmenstrual age (PMA), is a vital indicator of cerebral maturation, although preliminary, less defined cycling may be noted as early as 24–25 weeks. The primary objective of this dissertation is to differentiate between various sleep states, active sleep I (N_1), active sleep II (REM), quiet sleep I (N_{II}), quiet sleep II (N_{III}), and wakefulness (W_S), utilising just a few of EEG channels for sleep analysis.

EEG Relation with Sleep States: Newborns spend a large fraction of their early life asleep, with healthy full-term infants typically sleeping 16 to 18 hours per day [62]. This prolonged sleep is far from a passive resting period; it is accompanied by intense neurological and physiological activity [63; 64]. Numerous studies emphasize that neonatal sleep plays a fundamental role in the maturation of cognitive, psychomotor, and behavioural capacities [65; 66; 67]. Accordingly, systematic evaluation of sleep in newborns is vital for assessing brain functional integrity and for characterizing sleep patterns, particularly in infants at increased risk for conditions such as sudden infant death syndrome (SIDS) and sleep apnea [68; 69].

EEG activity in neonates differs markedly from that observed in adults. In particular, the amplitude of neonatal EEG signals is generally much lower. Over the first year of life (1–12 months), the EEG background undergoes notable developmental changes. From around two months of age, the posterior dominant rhythm, considered an early form of the alpha rhythm, begins to appear. Across development, the proportion of electroencephalographic power in the alpha range increases from essentially 0 % at birth to approximately 70 % in adulthood. The dominant frequency is initially around 3– Hz, increases to 4–5 Hz by six months, and reaches about 8.5 Hz by roughly 16 years of age. Asynchronous sleep spindles usually become evident between 2 and 3 months of age and persist, with ongoing maturation, between 6 and 12 months. These spindles typically last 10–15 seconds, and the period of asynchrony between them ranges from 1 to 5 seconds. K-complexes and V-waves emerge between 2 and 5 months, followed by additional maturational refinements throughout the first three years of life [70].

Bio-Insights of Neonatal Sleep EEG: The neonatal sleep EEG patterns, as classified by the American Academy of Sleep Medicine (AASM) Manual, provide key insights into different sleep stages in newborns, including $Q_S$and Wake/Active Sleep ($\mathrm{A_S}$). The key EEG patterns associated with each stage are outlined below:

Quiet Sleep:

- **Trace Alternant (TA):** This pattern is characterised by bursts of high-voltage delta activity (50 μV) alternating with periods of lower amplitude (25–50 μV) theta activity (4–7 Hz). The intervals between bursts, known as *inter-burst intervals (IBIs)*, increase with age, signalling developmental changes in the brain.
- **High Voltage Slow (HVS):** This pattern involves continuous high-voltage delta activity (100–150 μV at 1–3 Hz) that often shows a central or occipital predominance. During this stage, there is significant development of the *autonomous nervous system (ANS)*, which is crucial for physiological regulation during Quiet Sleep.

Wake/Rarely $\mathrm{A_S}$:

- **Mixed (M):** A pattern in which the *background* is low-voltage and mixed-frequency but contains intermittent higher-amplitude slow activity. Practically, the baseline may look LVI-like (often $< 50\,\mu$V much of the time), while *superimposed* delta components can intermittently exceed $100\,\mu$V (such as 2–4 Hz), especially around arousals/transitions or in some active-sleep epochs.

Wake/$\mathrm{A_S}$:

- **Low Voltage Irregular (LVI):** This stage involves continuous low-voltage, mixed-frequency activity dominated by delta and theta waves. The irregular theta activity (25–50 μV, 4–7 Hz) is combined with low-amplitude delta waves (1–3 Hz). This stage reflects the ongoing development of the *central nervous system (CNS)* during $\mathrm{A_S}$, highlighting its importance in brain maturation.

Each EEG pattern provides a valuable window into the neurological development of neonates. Monitoring stages such as Q_S and A_S is essential, as these stages are linked to the maturation of critical systems, including the ANS and CNS. Understanding these EEG patterns provides key insights into the functional and developmental status of newborns.

Clinical Significance and Interpretability: Neonatal sleep stages are often categorised into A_S, Q_S, and W_S. A_S and Q_S are further categorised into N_I, REM-II, N_{II}, and N_{III}. In newborn growth and development, these stages serve as a means to evaluate brain maturity, diagnose health conditions, and strategise interventions. Transitional sleep, characterised by a combination of A_S and Q_S, typically arises during state transitions and diminishes in frequency with a child's development. W_S is characterised by wide eyes, irregular respiration, and higher muscle tone. It facilitates sensory exploration, attachment, and nourishment, which are essential for early cognitive and physical growth.

A_S, specifically REM-II, is characterised by irregular respiration, rapid eye movements, and diminished muscular tone. This phase is essential for brain development, the integration of sensory and motor functions, and the formation of neural connections that support cognitive and motor advancement. Clinically, disturbances in A_S may signify developmental delays or neurological disorders, emphasising its significance in the surveillance of neonatal health [71].

Q_S, commonly referred to as non-rapid eye movement (NREM) sleep, is identifiable by rhythmic respiration, a consistent heart rate, and high-voltage slow electroencephalography (EEG) patterns, including alternating traces. This phase facilitates restorative processes, energy preservation, and immunological function, acting as an indicator of the brain's and thalamocortical connections. Irregularities in Q_S, including disrupted sleep or erratic respiration, may correlate with hypoxia, cerebral damage, or other medical conditions [71; 72].

Transitional (T) sleep transpires during the transitions between A_S and Q_S, exhibiting attributes of both states. It manifests in the early stages of newborn life and progressively diminishes with maturation. Monitoring T sleep reflects the dynamic characteristics of newborn sleep and its continuous maturation [71; 72].

In clinical practice, newborn sleep phases can serve as diagnostic indicators of neurological and systemic health. Abnormalities in standard sleep patterns, including excessive A_S or interrupted Q_S, may indicate developmental disorders, cerebral injuries, or systemic malfunctions. Monitoring sleep stages helps healthcare providers evaluate brain maturation, guide therapeutic actions, and enhance neurodevelopmental outcomes, particularly for neonates in critical care [71; 72].

Motivation and Challenges: The analysis of neonatal EEG signals presents unique challenges due to these recordings' high variability and noise. Neonatal sleep differs significantly from adult sleep, not only in its stages but also in its physiological characteristics. In contrast, adult sleep stages are typically divided into REM and non-REM (NREM), with NREM further classified into stages NREM1, NREM2, and NREM3 (recently simplified from NREM3 and NREM4) [73], neonatal sleep is categorised primarily into A_S (A_S) and quiet sleep (Q_S). A transitional state, referred to as indeterminate sleep (I_S), occurs between these stages, further complicating the classification process [73]. These complexities in accurately classifying neonatal sleep stages due to signal variability and noise serve as key motivations for this research, driving the need for improved analysis techniques.

Key differences between neonatal and adult sleep include:

- **Sleep Duration**: Neonates typically sleep for 17-18 hours a day, accounting for 70 % of their daily activity, compared to adults who sleep for 7-9 hours, or about 16-29 % of their day. Unlike adults, neonates have no established circadian rhythms to regulate their sleep patterns.

- **Sleep Spindles**: Sleep spindles, which play a crucial role in memory consolidation in adults, are absent in neonates and only begin to appear after 42 weeks of gestational age (GA) [74].

- **Sleep Cycle Duration**: The sleep cycle duration in neonates is approximately 50-60 minutes, significantly shorter than the 80-110 minutes typical of adult sleep cycles.

- **REM and NREM Sleep Distribution**: At 28 weeks GA, A_S constitutes 80 % of the total sleep time (TST), Q_S 18 %, and indeterminate sleep (I_S) 2 %. By 40 weeks GA, these distributions shift to 57 % A_S, 32 % Q_S, and 11 % I_S.

- **Brain Development and EEG Artefacts**: Neonates are in a rapid and dynamic brain development phase, making it difficult to establish consistent classification features. Furthermore, EEG data in neonates are often contaminated by artefacts from muscle movements, eye blinks, and equipment noise, which complicates the analysis and can lead to classification errors [75].

- **Standardisation of EEG Recording and Interpretation**: The lack of standardised protocols for recording and interpreting neonatal EEG signals contributes to variability in data quality and hinders the development of reliable classification models [76; 57]. Visual interpretation of EEG signals remains the gold standard in clinical practice. However, this process is inherently complex and subject to variability in expertise, experience, and fatigue, which can introduce subjectivity and affect the accuracy of interpretations. Additionally, the need for round-the-clock availability of EEG experts at every NICU presents a significant logistical challenge.

Current methods for staging neonatal sleep rely heavily on multiple EEG channels. Neonatal PSG often uses multiple EEG derivations (and other channels) because infant EEG is discontinuous, and staging relies on combining visual/physiological cues. More channels mean more wires/adhesives (practical burden) and more data to transmit/store. Skin irritation with prolonged EEG is a documented risk, making fewer-lead solutions attractive when feasible [71; 9]. Furthermore, existing approaches to neonatal sleep stage classification are hindered by their inherent subjectivity, time-consuming nature, and inter- and intra-rater variability. Analysing neonatal EEG signals presents unique challenges compared to those of adults. A combination of advanced signal processing with machine learning and the Internet of Medical Things (IoMT) offers promising solutions in various domains [30; 74], particularly revolutionising healthcare [77; 78; 79]. The application of IoMT for continuous, non-invasive monitoring of physiological signals, when coupled with edge-cloud computing [80; 81], offers a novel approach to the early detection and analysis of health parameters. This technological advancement aligns with the critical need for improved neonatal healthcare strategies [82]. However, an IoT-based system requires low computational demand, data efficiency, energy efficiency, and streamlined data acquisition.

To address these requirements, in **publication III**, we propose an innovative automated classification approach that integrates multi-view feature fusion, *AdaptiSelect*-based feature optimisation, the smart cloud data transfer and reconstruction (STREAM) module, and a rotational ensemble stacking model. The data reduction module significantly enhances edge-cloud systems' performance in IoT-based healthcare environments by reducing data transmission by a factor of 153.6 through efficient feature selection and compact data packet formation. This module ensures minimal bandwidth usage, reduces the computational load on resource-constrained edge devices, and lowers cloud storage requirements while maintaining full data reconstruction. The dataset used in this research combines two large Datasets collected over a four-year period from the Children's Hospital, Fudan University, Shanghai. A unique set of 315 features was extracted from each epoch of a single channel using flexible analytical wavelet transform (FAWT), dual-tree complex wavelet transform (DTCWT), enhanced covariance (ECOV), and spectral features based on α, β, θ, and δ brain waves. These features were refined using *AdaptiSelect*, which enabled achieving higher performance than previous published work through 10-fold cross-validation. Additionally, Leave-One-Subject-Out cross-validation (LOSO-CV) further demonstrates the effectiveness of the proposed approach as a generalised solution. Using both single and multichannel setups, the proposed approach outperforms the most significant **state-of-the-art methods** in neonatal sleep analysis.

1.2.6 Emotion Analysis: Minimal Sensing

Emotion is defined as a psychological reaction generated by both external stimuli and internal cognitive processes, which is accompanied by a variety of physiological changes in the human body. Also, mood is generally characterised as a dominant, conscious emotional state at a specific moment in time [83]. While there are many approaches to classifying emotions, one widely accepted and useful framework in psychology is the two-dimensional model of emotions. Despite its simplicity, this model offers a valuable tool for analysing emotional states and understanding their functional roles in everyday life. The relationship between basic emotions and the valence–arousal dimensions is illustrated in Fig. 5 . Emotions strongly influence both the physiological and psychological aspects of human life. Positive emotions promote improved health and productivity, but negative emotions can lead to a variety of health issues, especially if prolonged [84].

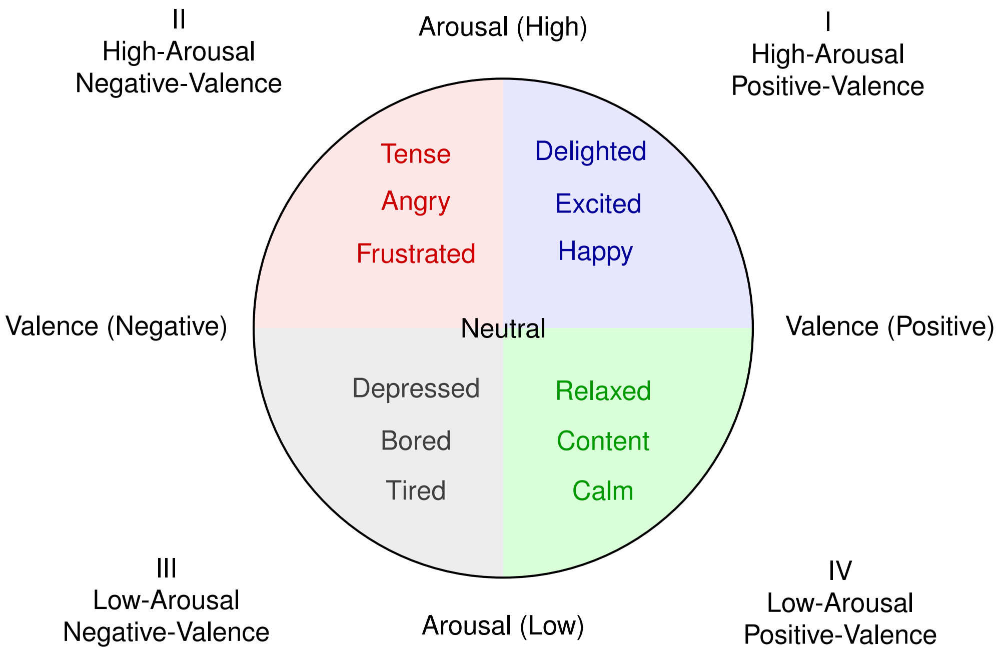

Figure 5. 2D Valence and arousal model together with several basic emotions. (**Publication V**)

To assess human emotion with *minimal sensing*, prioritisation is given to physiological signals that are information-rich, low power, and easy to acquire in ambulatory settings, most commonly single–lead ECG for cardiac dynamics and electrodermal activity (EDA; often called galvanic skin response, GSR) for sympathetic arousal. Recent review studies [85; 86; 87; 88], have highlighted the importance of physiological signals for emotion recognition, pointing out their reliability in comparison to speech- or facial-based techniques. For this reason, many studies have focused on physiological signals, particularly multimodal approaches that combine various physiological data obtained from biosensors, such as ECG, EEG, EMG, EDA, or GSR, PPG, blood volume pressure, and respiratory inductive PSG. While multimodal recognition of emotions often produces better results, the unimodal technique has the advantages of faster processing and easier data collection [89]. These modalities are well–established in affective computing and clinical psychophysiology, and have been validated across laboratory and real–world contexts [90; 91; 92; 93; 94; 95; 96; 97; 98; 99; 100].

Importance of Emotions Analysis:

Negative emotions are linked to the onset of neurodegenerative diseases and dementia. In Alzheimer's disease, prolonged negative patterns (repetitive negative thinking) correlate with increased amyloid/tau accumulation and accelerated cognitive deterioration, indicating a possibly alterable risk for dementia [101]. Behavioural and psychological symptoms of dementia, including sadness, apathy, agitation, delusions, and anxiety, impact up to 90 % of patients and frequently precipitate institutionalisation, highlighting the necessity for continuous monitoring of emotional states [102]. Positive emotions, such as gratitude, amusement, and tenderness, activate reward pathways and neuromodulators like serotonin and dopamine, thereby enhancing cognitive flexibility and resilience. The broaden-and-build theory posits that this leads to an expansion of thought–action repertoires and enduring resources [103]. To complement this perspective, emotion neuroscience studies show that positive affect increases functional connectivity in prefrontal and default-mode networks, thereby enhancing cognitive reserve, whereas negative affect reduces prefrontal regulatory control and increases amygdala responsivity. In contrast, prolonged negative emotions activate amygdala/insula circuits and stress-related physiology; persistently increased stress hormones hinder cognitive function and heighten susceptibility to mental health issues [104]. Together, these findings emphasise the clinical relevance of continuously monitoring emotional states, especially in populations vulnerable to cognitive decline.

Challenges: Although wearables provide non-invasive, continuous physiological monitoring, which is essential when self-reporting is inconsistent, especially in cases of dementia, practical limitations persist. Power constraints and Bluetooth Low Energy bandwidth restrict high-rate, multi-stream sensing. Simultaneous high frequency streams may result in packet loss and battery depletion, as evidenced by previous studies and commercial devices [105; 106; 80]. These limitations directly affect the feasibility of real-time affective monitoring, where continuous, uninterrupted data are required for reliable prediction. Thus, reducing sensing and computing is essential for reliable, real-time applications and becomes a key factor in designing solutions that can operate robustly in daily life settings.

Furthermore, in the case of dementia diseases, there are over hundred of types of dementia, and each person living with dementia has different experiences and symptom progressions. This variability reinforces the need for personalised solutions, where models learn from a subject's own physiological patterns rather than relying solely on population-level generalisations. Personalisation is particularly relevant in emotion recognition because autonomic physiology varies strongly across individuals; baseline cardiac variability, stress reactivity, and emotional expressivity differ widely in dementia populations. In this context, personalised models could be more optimal and effective, enabling the model to adapt to individual differences and predict emotional or other health outcomes with higher reliability.

Considering these points, personalised and generalised machine-learning models were evaluated for binary emotion classification (positive vs. negative) via wearable biosignals, aiming for a minimal-sensing architecture that employs a single physiological channel. Our pipeline prioritises multi-domain feature extraction with lightweight hybrid feature selection to optimise the feature set while minimising computational expense. We assess interpretable, resource-efficient classifiers designed for embedded and IoT-based deployment, which is particularly important for cognitively disabled populations, where unobtrusive and simpler solutions are crucial. By linking emotional neuroscience, dementia-specific variability, and real-world wearable constraints, this work addresses both the clinical relevance and the technical feasibility of emotion recognition under minimal sensing conditions.

In **publication IV**, we propose a lightweight, resource-efficient machine learning approach for binary emotion classification, distinguishing between negative (sadness, disgust, anger) and positive (amusement, tenderness, gratitude) affective states using only ECG signals. The method is designed for deployment in resource constrained systems, such as for the IoT devices, by reducing battery consumption and cloud data transmission through the avoidance of computationally expensive multimodal inputs. Our approach integrates multidomain feature extraction, selective feature fusion, and a voting classifier. We evaluated it using a participant-exclusive generalised model and a participant-inclusive personalised model. The personalised model achieved the best performance, outperforming the generalised model. Comparisons on the POPANE dataset demonstrate that our method consistently outperforms the standard models commonly used in this domain. This work underscores the effectiveness of personalised models for emotion recognition and their suitability for wearable devices that demand accurate, low-power, real-time emotion tracking.

1.3 Aims of the Thesis

The central objective of this thesis is to design and assess computationally efficient AI techniques for analysing neuroimaging and physiological signals, tailored to clinically relevant scenarios with limited resources. The research centres on three illustrative applications spanning the neuro–cardio–sleep spectrum: brain tumour assessment using MRI, neonatal sleep stage classification from EEG, and emotion detection based on wearable ECG. More specifically, the thesis pursues the following aims:

- **Aim 1:** To design lightweight, lesion-aware deep learning architectures for brain tumour classification from MRI, balancing diagnostic performance with computational efficiency and inference-time feasibility for real-world deployment **(Publications I-II)**.
- **Aim 2:** To develop multiview feature-fusion and channel-reduction methods for neonatal EEG sleep staging, utilising spectral and time–frequency representations to enable reliable four-stage classification with fewer electrodes, making the montages more feasible for routine NICU use **(Publication III)**.
- **Aim 3:** To develop emotion recognition from minimal wearable sensing using the POPANE dataset, which provides single-lead ECG recorded in a modified Lead II configuration at 1000 Hz; to build a low-complexity pipeline combining multidomain feature extraction, hybrid feature selection, and ensemble learning; and to compare subject-independent (generalised) and subject-specific (personalised) models for the real-time emotion-aware applications **(Publication IV)**.
- **Aim 4:** Highlight the trade-offs between performance and efficiency, and practical considerations for edge–cloud deployment.

1.4 Structure of the Thesis

This thesis is organised as a compilation of five peer-reviewed publications, framed by introductory and synthesis chapters.

- **Chapter 2** describes the datasets used throughout the thesis. It presents the publicly available MRI datasets for brain tumour analysis **(Publication I and II)**, the neonatal EEG dataset **(Publication III)** for four-stage sleep classification from Children's Hospital, Fudan University, Shanghai, and the ECG-based emotion dataset (POPANE dataset used in **Publication IV**). Data collection settings, key signal characteristics, and relevant preprocessing considerations are summarised.
- **Chapter 3** outlines a generic AI workflow for healthcare applications. It reviews typical pipelines for conventional machine learning and deep learning in medical imaging and physiological signal analysis, with a particular focus on minimal wearable sensing. The chapter also provides concise overviews of **Publications I–IV**, linking each study to the overarching thesis aims.
- **Chapter 4** presents and synthesises the main results from **Publications I–IV**. It summarises the quantitative findings on brain tumour MRI classification, neonatal sleep staging with multiview EEG features and reduced channel sets,

and ECG-based emotion recognition. The chapter compares generalised versus personalised models, analyses robustness to noise and artefacts, and discusses computational complexity and inference-time constraints across the different case studies.

- **Chapter 5** discusses the overall scientific and practical contributions of the thesis. It integrates insights from all four publications, reflects on their implications for deployable AI in brain imaging and physiological monitoring, and outlines limitations and directions for future research, including edge–cloud architectures and translational pathways toward clinical and real-world use.

2 Datasets

2.1 MRI Datasets for Brain-Tumour Classification

2.1.1 Dataset I (Publication I & II)

The Kaggle "Brain MRI data for Diagnosing Brain Tumour" collection [107] provides a baseline for binary classification (tumour vs. non-tumour). It contains 3060 2D slices (1500 tumour, 1500 non-tumour; 60 unlabelled excluded). We used a stratified split: $70\,\%$ training and $30\,\%$ held out for validation/testing. Image names were organised by class prefix: "y*" (tumour) and "no*" (non-tumour).

2.1.2 Dataset II (Publication I & II)

Dataset II [108] was originally curated for segmentation with masks; for classification, the masks were omitted. The set contains 2501 images (950 tumour, 1551 non-tumour). We used a stratified $70\,\%$/$30\,\%$ train/holdout split and the same class prefixing ("y*", "no*").

2.1.3 Dataset III (Publication I & II; Combined)

Dataset III merges Datasets I and II to increase diversity, yielding 5501 images (2450 tumour, 3051 non-tumour). A stratified $70\,\%$ / $30\,\%$ split was applied, explicitly balancing contributions from the two sources across training, validation, and test. The final test set contained 900 images (450 from Dataset I and 450 from Dataset II).

2.2 Neonatal EEG Dataset (Publication III)

Table 1 summarises cohort and signal specifications. These data were used in **Publication III**.

Participant information On average, neonates were born at 38.3 ± 1.8 weeks of gestation; data collection occurred at a postmenstrual age of 40.5 ± 1.7 weeks. Mean weight was $3.3 \pm 0.6\,\mathrm{kg}$. Mean sleep duration was 86.5 ± 34.4 minutes, and wakefulness averaged 43.0 ± 34.5 minutes.

Table 1. Neonatal cohort and recording specifications.

Term	**Detail**
Sex (boys:girls)	32:32
Gestational age (weeks)	38.3 ± 1.8
Postmenstrual age (weeks)	40.5 ± 1.7
Weight (kg)	3.3 ± 0.6
Sleep stage counts	
Awake (W_S)	5514
Active Sleep I (N_1)	4785
Active Sleep II (REM–II)	755
Quiet Sleep I (N_{II})	1247
Quiet Sleep II (N_{III})	4502
Reason for inclusion	Pneumonia, jaundice, etc.
EEG channels used	F3, F4, C3, C4, T3, T4, P3, P4
Sampling rate	$500\,\mathrm{Hz}$

Notes: boys:girls = biological sex counts; weeks reported as mean $\pm$SD. Stage labels follow the study's internal convention.

Inclusion criteria Clinical indications included hyperbilirubinaemia, sepsis, and other routine NICU admission reasons.

Data collection Physiological signals (EEG, EOG, EMG, ECG) were acquired on a Nicolet system at $500\,\mathrm{Hz}$. EEG electrodes included Fp1, Fp2, F3, F4, C3, C4, P3, P4, T3, and T4 with Cz as reference; data were resampled to $128\,\mathrm{Hz}$ for analysis to reduce redundancy.

Sleep stage annotation Neonatologists specialised in neonatal sleep staged the recordings manually; these labels served as the reference standard for evaluation.

Ethical approval The study protocol was approved by the Research Ethics Committee of Fudan University, Shanghai, China, approval number (2017) 89.

2.3 POPANE Emotion Dataset (Publication IV)

We utilise the publicly available POPANE dataset [109], which comprises approximately 725 hours of multimodal psychophysiological recordings from 1157 healthy young adults collected across seven independent studies. In line with affective science, physiological activity is a core component of emotional responses alongside subjective experience and behaviour. POPANE was designed to characterise both positive such as amusement, tenderness, and gratitude. and negative such as anger, disgust, fear, sadness, threat) affective states during rest and controlled emotion elicitation.

Across studies, affect was recorded continuously during a resting baseline and during tasks that reliably evoke emotions, including film clips, static pictures, speech preparation, and expressive writing. Physiological signals include ECG, impedance cardiography (ICG), EDA, PPG/blood volume pulse (BVP), respiration, and skin temperature. Each study is organised in a separate folder; within a study, data for each participant are provided as: (a) a full laboratory recording, for example `123_All.csv`); (b) a separate baseline file, such as `123_Baseline.csv`); and (c) one or more emotion-elicitation files, such as `123_Manipulation1.csv`). Files contain multiple channels, such as valence annotations, ECG, EDA, PPG/BVP, and a marker channel. The accompanying `metadata.xlsx` file maps markers to specific emotion conditions.

In this thesis, we analyse *ECG only* to perform classification of (positive vs. negative). This minimal-sensing choice aligns with our deployment goals: it reduces battery consumption on wearables and lowers data transmission to the cloud while retaining discriminative autonomic information relevant to affect.

3 General Workflow in AI for Healthcare

A typical healthcare-oriented AI research pipeline comprises numerous organised phases to ensure clinically useful, technically robust, and deployable models under real-world constraints, as shown in Figures 6 and 7. This technique is applied to brain tumour MRI classification, newborn sleep staging, and minimal-sensing emotion recognition in this thesis.

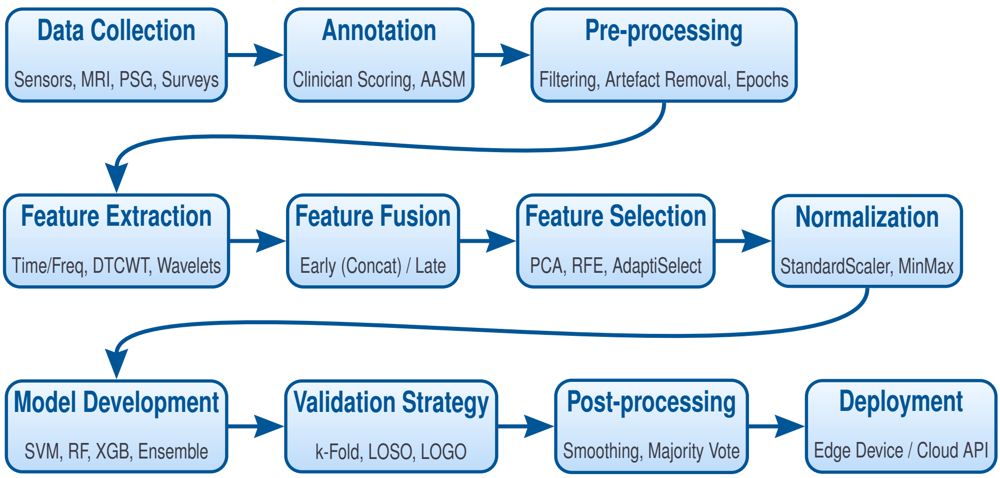

Figure 6. Flow diagram for models performing preprocessing and feature extraction.

3.0.1 Data Collection

The workflow begins with data acquisition, either through new recordings from human subjects or publicly available Datasets. In this thesis, for example:

- Brain tumour classification uses publicly available MRI Datasets to validate the fuzzy-logic CNN models.
- Neonatal sleep staging relies on multichannel EEG recorded through PSG.
- Emotion recognition uses wearable-sensing modalities such as ECG and GSR, where ECG captures cardiac autonomic dynamics, and GSR reflects sympathetic arousal.

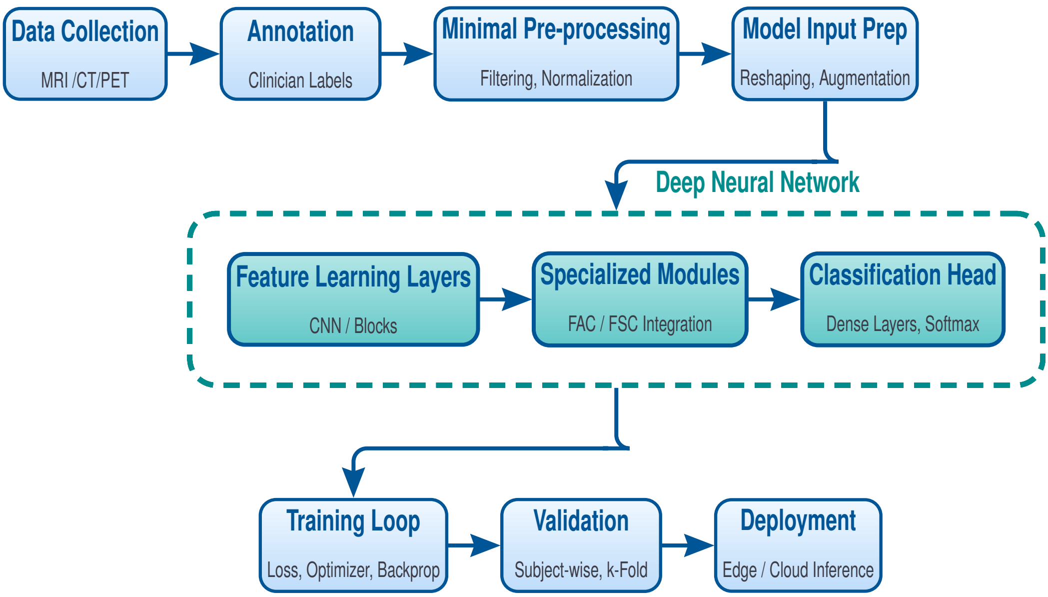

Figure 7. Deep Learning Pipeline integrated with specialised feature learning (FAC/FSC)

Each physiological signal has unique characteristics:

- **EEG** provides rich frequency-specific information and is preferred for sleep staging.
- **ECG** reflects heart-rate modulation strongly linked to emotional arousal.
- **MRI/CT** reveal anatomical brain structures important for tumour localisation.

Together, these modalities illustrate the diversity of data types used in AI for healthcare.

3.0.2 Labelling and Annotation

Following data collection, expert annotation is essential. In MRI, radiologists label the presence or type of a tumour. When annotations from multiple experts are available, inter-rater agreement can be evaluated using measures such as Cohen's Kappa (κ). Clinicians annotate 30-second EEG epochs for sleep staging in accordance with AASM recommendations, although length may vary based on application. In emotion datasets, labels are derived from stimulus metadata, experimental techniques, or subjective self-reports. The model's top performance constraint is directly determined by high-quality labels, whereas noisy labels propagate errors throughout the pipeline.

3.0.3 Data Preparation and Pre-processing

Pre-processing converts raw data into a form suitable for modelling. Depending on the modality, this may include:

- **Filtering and signal pre-processing:** low-pass, high-pass, and notch filtering for ECG/EEG; MSPCA for multiscale EEG denoising; and baseline correction for wearable signals.
- **Artefact detection:** removal of segments affected by movement or sensor noise.
- **MRI pre-processing:** timage augmentation using random horizontal and vertical flips, random rotations (up to 20°), and color jitter. All MRI images are normalised using ImageNet mean and standard deviation values, resized to 224×224 or 128×128 pixels depending on GPU memory, and reflection padding is applied before resizing to preserve edge information. Validation and test images are not augmented; they are only resized and normalised.
- **Segmentation into epochs:**
  - Sleep staging typically uses epochs of 30 s.
  - Real-time emotion recognition advantages from short windows, such as (10 s) to reduce alerting latency.
  - MRI analysis may use patches or slices, depending on the tumour's resolution requirements.

Shorter windows may compromise accuracy, but they are crucial for prompt responses, particularly in neonatal care, dementia surveillance, and wearable edge-computing contexts.

3.0.4 Edge vs. Cloud Processing

Modern healthcare AI often uses edge–cloud architectures:

- **Edge computing** processes sensitive or time-critical data locally, reducing latency and bandwidth requirements. This demands computationally efficient models such as the lightweight fuzzy CNN architectures (FAC and FSC) proposed in this thesis.
- **Cloud computing** handles tasks needing greater computational resources, and in this case, data are transmitted to a remote server for inference or training.

- **Hybrid systems** split the pipeline such that filtering, feature extraction, and packet formation occur at the edge, while model inference or extended analytics run in the cloud.

The models (FAC, FSC, ensemble) developed in this thesis are well-suited to both edge and cloud-oriented workflows, owing to their compact architectures, parameter-efficient design, and reduced requirements for energy, memory, and data transmission

3.0.5 Feature Extraction

In feature-based machine learning pipelines, meaningful features are typically computed using signal processing methods [**?** 106]. Examples used in this thesis include:

- **Time-domain features:** mean, standard deviation, HRV metrics.
- **Frequency-domain features:** PSD bands, LF/HF components.
- **Wavelet-based transforms:** FAWT, DTCWT, MSPCA.
- **Autoregressive descriptors:** ECOV spectral features.

Each of these captures complementary physiological information: wavelets deliver time–frequency localisation; HRV quantifies autonomic nervous system activity; and spectral features summarise rhythmic structure.

3.0.6 Feature Fusion and Selection

Feature fusion can follow two strategies:

- **Early fusion:** concatenate all feature groups and then perform feature selection.
- **Late fusion:** apply feature selection to each feature group independently, then combine the reduced sets.

Both approaches aim to reduce redundancy and computational load, particularly important for edge deployment. A key methodological requirement is that **feature selection must be fitted only on the training data**. The learned transformation is then applied to validation and test sets to avoid data leakage.

3.0.7 Model Development

Common machine-learning models used in healthcare include:

- Support Vector Machines (SVM),
- Random Forests and Extra Trees,
- Gradient Boosting Machines (GBM, XGBoost, LightGBM),
- Naïve Bayes,
- k-Nearest Neighbours (KNN),
- Multilayer Perceptrons (MLP).

Ensemble techniques such as stacking, soft/hard voting, and bagging often outperform individual models by combining complementary decision boundaries. In **Publication IV**, a custom ensemble (EnsemNet) achieved the best performance. Although deep learning models automatically extract informative features, they typically depend on large datasets and substantial computational capacity. Their reduced interpretability remains a major concern, reinforcing the need for explainable techniques and, in some applications, favouring simpler machine-learning models that offer greater transparency.

3.0.8 Data Splitting and Validation

Robust evaluation involves carefully designed splits, such as:

- Train/validation/test splits for hyperparameter optimisation,
- k-Fold cross-validation for stable performance estimation,
- Leave-One-Subject-Out (LOSO) for personalised modelling (subject independent),
- Leave-One-Group-Out (LOGO) for cross-site oe group generalisation,
- Random splits, used only when subject leakage is not a concern.

Different publications in this thesis employ validation strategies tailored to the dataset structure and research objective. In Publications I and II, stratified train/validation/test splits are used for binary brain-tumour classification from MRI. In Publication III, both cross-validation and leave-one-subject-out validation are used to assess neonatal sleep-stage classification performance and subject-level generalisability. In Publication IV, separate validation settings were used for personalised and generalised ECG-based emotion recognition. These strategies were selected to ensure fair evaluation and to match the intended application of each study.

3.0.9 Post-processing

Post-processing can include probability smoothing, threshold calibration, majority voting, or temporal filtering. However, heavy post-processing may hinder real-time applicability. For edge-based use cases such as emotion alerts or neonatal monitoring, minimal or no post-processing is preferred.

These steps form a complete pipeline from raw data to clinically meaningful AI output. Across all publications, this thesis emphasises low-computational-cost models, robustness across subjects and modalities, and compatibility with edge–cloud deployment, ensuring the feasibility of these methods in real healthcare environments.

3.1 Fuzzy Atrous Convolution for Brain Tumour MRI

In **Publication I**, we address binary brain-tumour classification in MR images using a lightweight convolutional architecture (FAC) that enlarges the receptive field (via dilations) without discarding input samples, using fuzzy memberships at the zero entries of dilated kernels. The full pipeline covers dataset preparation, augmentation, FAC-based feature extraction (TOFU/MOFU), and final classification. By incorporating a fuzzy membership function into the existing convolution process, the FAC can preserve an identity mapping from the input data [110]. It enables unrestricted data flow and maximises gradient transfer. A convolution function is an operation that multiplies, adds, or accumulates. When a CNN model is convoluted, the input is split into the corresponding sliding windows. At every sliding step, every element is accumulated or added after the convolution kernel is multiplied element-wise [111].

TOFU (Top of the Funnel). A dense dilated block extracts high-resolution features using three dilated convolutions with concatenation and a 1×1 compressor, producing rich early representations with minimal depth. The implementation of this block is given in Algorithm II in **Publication I**.

MOFU (Middle of the Funnel). Three FAC layers downsample aggressively with matched stride/dilation values $\{2, 3, 5\}$, reducing maps from $512{\times}512 \to 15{\times}15$ or $224{\times}224 \to 5{\times}5$, while preserving context via FAC. A random channel permutation between TOFU and MOFU increases diversity. The implementation of this block is given in Algorithm III in **Publication I**.

Classifier (Bottom). Flattened MOFU output feeds a fully connected layer for binary prediction (tumour vs. non-tumour). The implementation of this block is given in Algorithm IV in **Publication I**.

3.2 Fuzzy Sigmoid Convolution for Brain Tumour MRI

In **Publication II**, we introduce FSC, an innovative convolutional layer that integrates fuzzy logic principles with convolutional neural networks. FSC improves the feature extraction abilities of traditional convolution layers by dynamically adjusting the contributions of various feature activation's through fuzzy membership functions based on sigmoid activation. The overall network structure is composed of three major components: TOFU blocks, MOFU blocks, and fully connected layers.

The FSC layer applies fuzzy membership functions to the convolution process, modulating each feature map through two sigmoid-based membership functions: *high membership* and *low membership*. These functions adjust the importance of individual features based on their activation values.

Given an input x passed through a convolution operation and batch normalisation, the fuzzy membership functions are defined as follows:

$$\text{high\_membership} = \sigma(x), \tag{3}$$

$$\text{low\_membership} = \sigma(-x), \tag{4}$$

where $\sigma(\cdot)$ is the sigmoid activation function.

The output of the FSC layer, denoted as o_{fsc}, is computed by combining the feature map x with the high and low membership functions as follows:

$$o_{\text{fsc}} = \text{high\_membership} \cdot x + \text{low\_membership} \cdot (1 - x). \tag{5}$$

This mechanism allows the network to emphasise more critical features while suppressing less relevant ones dynamically. After computing o_{fsc}, the result is passed through a ReLU activation function:

$$o_{\text{relu}} = \text{ReLU}(o_{\text{fsc}}). \tag{6}$$

TOFU: The TOFU block is designed to gradually enhance feature extraction by stacking multiple FSC layers with progressively larger receptive fields. Each FSC layer collects features from the previous layers. The final output of the TOFU block is produced by concatenating these feature maps and applying a compression step via a 1×1 convolution. The implementation of this block is given in Algorithm II in **Publication II**.

MOFU: In the MOFU block, the features extracted by the TOFU block are further refined. It employs downsampling and captures multi-scale features by applying several FSC layers with varying dilation rates, as given in Algorithm III in **Publication II**.

Bottom Layer: After feature extraction via the TOFU and MOFU blocks, the model uses global average pooling to reduce the feature maps to a 256-dimensional vector. This vector is passed through two fully connected layers with ReLU activation and dropout to prevent overfitting. The final layer then maps the output to the target binary class, completing the prediction as given in algorithm IV in **Publication II**.

3.3 Neonatal Sleep Analysis using EEG

In **Publication III**, we examine neonatal sleep analysis using EEG recorded via a PSG device, with the aim of designing a lightweight, deployment-minded pipeline that supports accurate sleep staging while remaining suitable for resource-constrained clinical environments. The diagrams in Fig. 8 illustrate the cloud implementation, while Fig. 9 presents the proposed IoMT architecture for edge-cloud structures. In the cloud implementation, data is transferred to the cloud, similar to our previous studies [112; 80]. However, to minimise data transfer, data packet formation is implemented in the edge-cloud structure, as shown in Fig. 9.

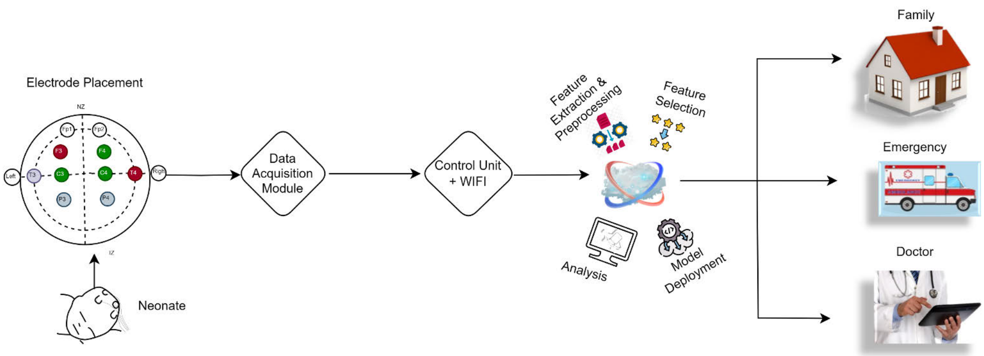

Figure 8. Implemented Cloud-Based Multiview EEG Signal Processing Framework for Neonatal Sleep Analysis Using AdaptiSelect and Ensemble Models

Raw EEG is preprocessed with finite impulse response (FIR) filtering (0.3–35 Hz), artefact screening, and segmented into 30 s epochs. To attenuate structured noise while preserving morphology, we apply multi-scale principle component analysis (MSPCA; Symlet-4, level = 8). We then extract a multiview feature set per epoch, comprising the Flexible Analytical Wavelet Transform (FAWT), Dual-Tree Complex Wavelet Transform (DTCWT), enhanced-covariance (ECOV) AR spectral features, and band-limited spectral statistics, which capture complementary time–frequency, autoregressive, and power-spectrum cues. From 315 features per channel epoch (95 FAWT, 130 DTCWT, 50 ECOV, 40 spectral), the *AdaptiSelect* module selects the most effective 122 features for single-channel, >900 across eight channels. We have also provided a comparison of the feature importance values of Multi-Scale Hierarchical Neural Network (MSHNN), SWT, DTCWT, and multiview methods.

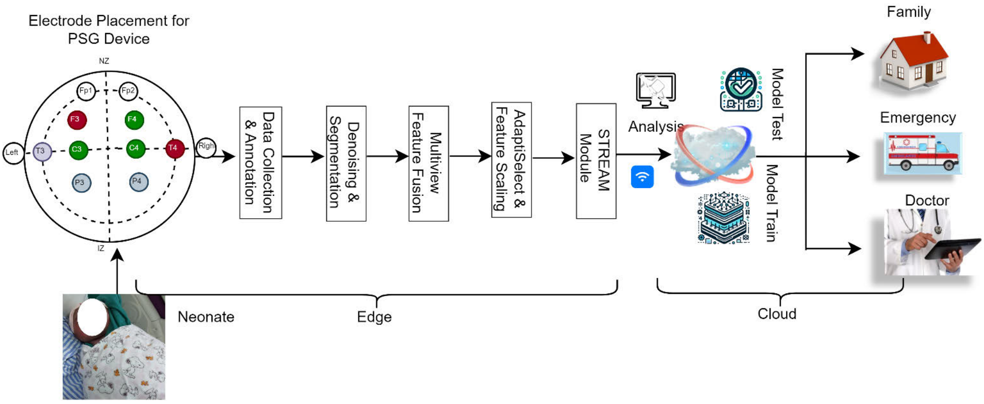

Figure 9. Proposed Edge-cloud-Based Multiview EEG Signal Processing Framework for Neonatal Sleep Analysis Using AdaptiSelect and Ensemble Models

Classification employs a rotation ensemble stacking design that combines Rotation Forest Extra Trees, Gradient Boosting, and Random Forest (as a meta-learner). Validation employs a stratified 10-fold CV for model development and LOGO holdouts for subject-wise generalisation. For edge/cloud efficiency, the STREAM module packages selected features into compact 5-feature packets, yielding $\sim 153.6\times$ reduction versus transmitting raw samples per epoch while retaining epoch identity for lossless reconstruction in the cloud. Overall, the multiview + AdaptiSelect + rotation-ensemble stack delivers excellent performance for the four-stage neonatal sleep classification with low computational and transmission cost and outperforms previous model development in the same domain.

3.4 Minimal Wearable Sensing for Emotions Analysis

In **Publication IV,** the methodology focuses on using ECG signals to classify emotions into positive and negative classes. To enable real-time and low-latency emotion detection, we chose a 10-second epoch length for segmentation. This decision enables a balance between the need for timely classification and the constraints of edge computing and wearable devices. Although shorter epochs can slightly reduce classification performance compared to longer windows, they enable near-real-time alerts, which are crucial in scenarios where immediate feedback is required. By segmenting into 10-second epochs, the system can deliver emotion classification and potential emergency alerts almost instantly, rather than waiting for longer windows that could delay intervention. The workflow involves a multi-stage preprocessing pipeline to clean the ECG data, including notch, high-pass, and low-pass filtering to remove noise and baseline drifts.

In terms of model development, we designed a streamlined pipeline that includes multi-domain feature extraction from time, frequency, and HRV domains, followed by a hybrid feature selection process to maintain computational efficiency. We experimented with several feature selection methods and proposed a hybrid feature selection approach to select the optimal method for emotion detection. We tested a range of machine learning classifiers and ultimately developed an ensemble model for its robust performance and adaptability. This approach is designed for both personalised and generalised models, recognising that in the case of dementia patients, there are multiple types of dementia, and each patient's experience can vary significantly. By incorporating both personalised and generalised modelling approaches, we can better tailor the emotion recognition system to individual variability, especially in populations with diverse and changing emotional responses. The proposed methodology offers a lightweight, real-time capable solution that can be deployed on wearable and edge devices, ensuring both efficiency and the flexibility to adapt to individual needs.

4 Summary of key findings and Discussion

Across **Publications I and II**, we performed systematic ablation studies to understand how architectural choices influence model behaviour and to evaluate performance under conditions that approximate real clinical variability. For brain–tumour MRI classification, both FAC and FSC were tested under three stress scenarios: (i) biased class splits, (ii) additive noise, and (iii) partial occlusion. The ablations varied in support parameters and model depth, such as the number of fuzzy blocks. These experiments demonstrated that moderate architectural depth, combined with appropriately tuned support values, offers the best balance between accuracy, stability, and robustness. Both FAC and FSC maintained high accuracy and F1 scores across all testing conditions, with only marginal performance degradation, indicating that the proposed fuzzy–convolutional modules can tolerate imbalance, noise, and missing information. We also benchmarked the proposed models against strong baselines, including transfer-learning backbones and classical machine-learning pipelines. FAC and FSC matched or exceeded state-of-the-art performance while using substantially fewer parameters, supporting their suitability for deployment in edge-cloud pipelines where computational efficiency is essential.

For **Publication III**, we performed a comprehensive analysis of feature importance, channel-reduction strategies, and ablation studies for EEG-based neonatal sleep staging. We evaluated multiple machine-learning models on complete PSG data (eight channels) and then progressively reduced the channel set to single- and dual-channel configurations. Using the stream module, we quantified the data reduction ratio. We demonstrated that the proposed method can significantly reduce transmission to the cloud while still allowing full reconstruction at the cloud side. The proposed feature-fusion strategy outperformed existing approaches, and we also reported execution time, feature-fusion latency, and packet-formation time as key factors for practical neonatal monitoring systems.

In **Publication IV**, we compared several feature-selection techniques with the proposed method and evaluated multiple machine-learning classifiers under both personalised and generalised settings for ECG-based emotion recognition. Across both settings, the proposed pipeline consistently outperformed standard approaches typically used for emotion-classification tasks, demonstrating its suitability for real-time, low-latency affective monitoring on wearable and edge devices.

4.0.1 Publication I: FAC for Brain–Tumour MRI

In **Publication I**, we evaluate the FAC architecture for binary brain tumour classification using three publicly available MRI Datasets (Datasets I–III). We examine robustness under biased test splits, additive noise, and partial occlusion, and conduct an ablation on the support parameter and network depth. **Publication I** provides comprehensive descriptions of the experimental technique and dataset. Performance under several conditions is provided in Fig. 10.

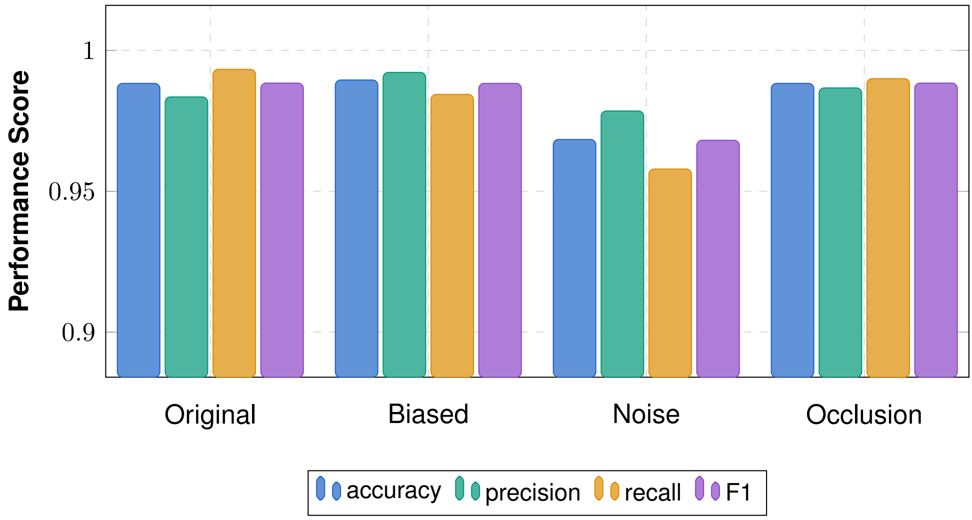

Figure 10. Performance of the FAC model under four evaluation conditions (original, biased split, Gaussian noise, partial occlusion). The consistently high accuracy, precision, recall, and F1-score highlight the robustness of the architecture to data imbalance and perturbations.

Dataset I-Original: With standard augmentation and early stopping, FAC achieved 0.9883 accuracy, an F1 score of 0.9884, and a Cohen's κ of 0.9767. These results were obtained using mixed-precision training and gradient accumulation, demonstrating an efficient and resource-aware training strategy.

Biased Split of Dataset I: As shown in Fig. 11, despite the imbalance, the model performed equally well as in the balanced data scenario, achieving a test loss of 0.0468, an accuracy of 0.9895, a precision of 0.9922, a recall of 0.9844, an F1 of 0.9883, and a κ of 0.9788.

Added Noise in Dataset I: Gaussian noise was introduced to evaluate the model's robustness under degraded imaging conditions. Using a 128×128 input and an effective batch size of 52 (via gradient accumulation), the training was capped at 200

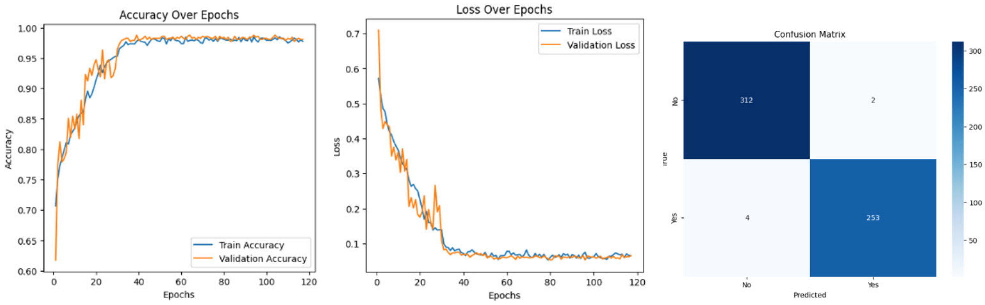

(a) accuracy over epochs **(b)** Loss over epochs **(c)** Confusion matrix

Figure 11. FAC under *biased split* on Dataset I . Training dynamics and final confusion matrix illustrate robustness to class imbalance.

epochs, and the model achieved an accuracy of 0.9684, precision of 0.9785, recall of 0.9579, F1 score of 0.9681, and $kappa$ of 0.9368. These results are reported in **Publication I**. A second experiment, using a larger 224×224 input, batch size of 32, and a patience value of 50, was trained for 139 epochs (early stopping, with a maximum limit of 200) and yielded improved performance, achieving a test accuracy of 0.9807, F1 score of 0.9807, and κ of 0.9614. The corresponding confusion matrix, learning curves and metric trajectories are presented in Fig. 12.

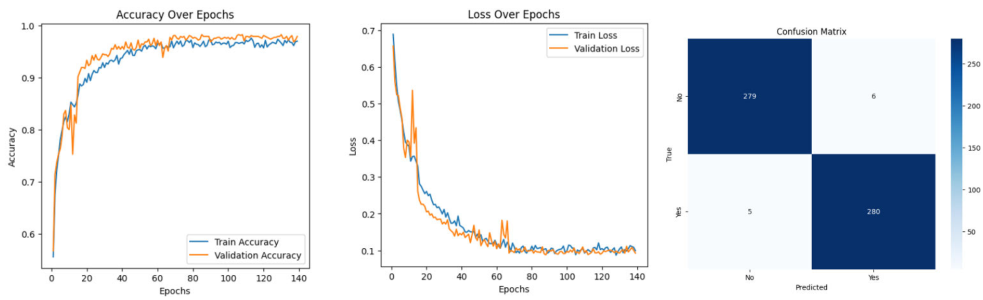

(a) accuracy over epochs **(b)** Loss over epochs **(c)** Confusion matrix

Figure 12. FAC evaluation under *added Gaussian noise* on Dataset I. Training and validation curves show stable convergence, and the confusion matrix reflects strong generalisation despite noise injection, demonstrating robustness across resolutions.

Performance on Dataset I with Simulated Partial Occlusion: To assess robustness to missing visual information, we introduced partial occlusions to images, simulating real-world conditions where parts of the image might be obscured during training, validation, and testing. Using a 224×224 input, a batch size of 52 (with gradient accumulation), and 26 for validation and testing, along with early stopping, the model achieved an accuracy of 0.9883, precision of 0.9867, recall of 0.9900, F1 score of 0.9884, and a κ of 0.9767. These results indicate that FAC maintains stable performance even when relevant image regions are partially obscured, as illustrated in Fig. 13.

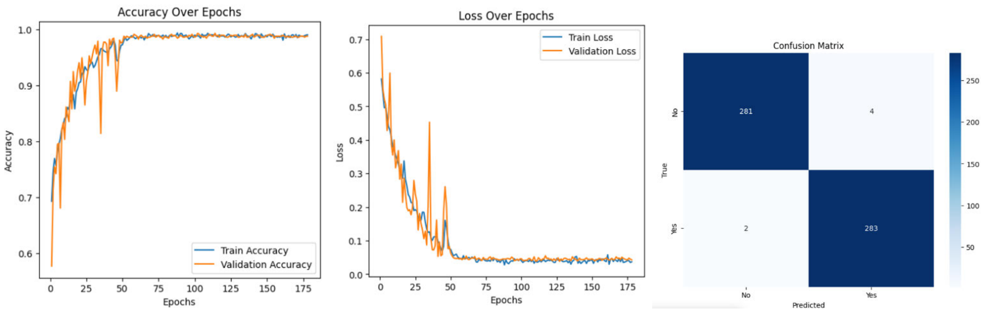

(a) accuracy over epochs **(b)** Loss over epochs **(c)** Confusion matrix

Figure 13. FAC evaluation under *Simulated Partial Occlusion* on Dataset I. Training and validation curves show stable convergence, and the confusion matrix reflects strong generalisation despite simulated Partial Occlusion injection, demonstrating robustness across resolutions.

In general, performance remains largely the same across class imbalance and occlusion, with only a limited drop under noise, aligning with the inductive bias of FAC towards prominent, spatially localisable signals.

Ablation: Support Parameter & Depth (Dataset III). A three-block FAC offers the most stable trade-off between accuracy and over-downsampling, achieving an accuracy of 0.9956 with three layers compared with 0.9936 for two layers. The choice of support parameter also matters: fixed values of $\mu \in \{0.5, 0.7\}$ remain competitive (accuracy between 0.9946 and 0.9956), while VEOC yields an accuracy of 0.9950, suggesting that per-channel adaptability is beneficial but not strictly necessary when the network depth is well chosen.

Comparison to Baselines (Dataset III). Against state-of-the-art transfer baselines trained at $224{\times}224$, such as VGG19 (0.9880 accuracy) and ResNet101 (0.9775 accuracy), FAC reaches an accuracy of 0.9956 with only **47.82K** parameters, smaller by several orders of magnitude than typical transfer-learning backbones (6.47–25.89M parameters). This closes the accuracy gap and improves computational efficiency, positioning FAC for edge/cloud deployment.

Operational Significance. (i) Stability to class imbalance and occlusion supports clinical use where sampling is imperfect, and artefacts occur; (ii) the controlled loss under noise motivates integrating denoise/augment or test-time ensembling in pipelines with known acquisition variability; (iii) parameter efficiency enables on-device triage and cost-effective scaling.

Computational efficiency and deployability. To evaluate deployment feasibility, we benchmarked inference speed and memory footprint using an input tensor,which represents a single image passed through the model during forward propagation. Across all compared architectures, the proposed FAC model exhibited the smallest memory footprint (0.19 MB) and the fastest per–image inference time (3.7 ms; ≈270 FPS). In contrast, widely used transfer learning backbones such as VGG16 (512 MB), VGG19 (532 MB), and ResNet50 (89 MB) are two to three orders of magnitude larger and substantially slower (7–12 ms per image).

For throughput benchmarking, the proposed model achieved 269.8 FPS, outperforming both lightweight networks (MobileNetV2: 134 FPS; EfficientNet-B0: 83.8 FPS) and heavier backbones (ResNet50: 130 FPS; VGG16: 105 FPS; DenseNet-121: 51.9 FPS). This represents approximately a 2× speed-up over MobileNetV2, 3× over VGG16, and more than 5× over DenseNet121, despite requiring significantly fewer parameters. These results demonstrate that the FAC architecture delivers state-of-the-art accuracy while meeting real-time constraints, making it highly suitable for edge, embedded, and IoT deployments where memory, latency, and power budgets are limited.

4.0.2 Publication II: FSC for Brain–Tumour MRI

Publication II evaluates the FSC architecture for binary brain tumour classification across three publicly available MRI Datasets (Datasets I–III), following the same reliability assessment protocol described in Section 4.0.1. The FSC model contains 0.21627 million parameters, which is larger than FAC (47,820 parameters), yet it consistently achieves higher classification performance. For example, on the original Dataset I, FSC achieves an accuracy of 0.9917, compared with 0.9883 for FAC. Under noisy conditions, FSC reaches 0.9702 versus 0.9684 for FAC, and in the biased split and partial occlusion scenarios, FSC achieves 0.9825 and 0.9877, respectively, outperforming FAC in all cases as provided in Publications I and II. A similar trend is observed for Datasets II and III. Figures 14, 15, and 16 provide additional visualisations of the FSC training behaviour, including accuracy and loss trends over epochs and the corresponding confusion matrices for each perturbation setting. Notably, the results in Fig. 14 show a slight performance improvement compared to those in Table II of Publication II. This improvement is due to using a higher input resolution (128 × 128) and increasing the early-stopping patience from 20 to 30 epochs, both of which helped stabilise convergence and reduce over-regularisation.

When comparing both proposed approaches from **Publications I and II**, FAC and FSC use substantially fewer parameters than state-of-the-art transfer learning

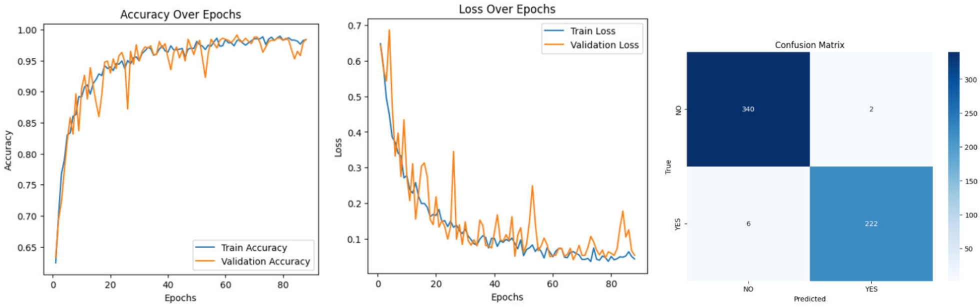

(a) accuracy over epochs **(b)** Loss over epochs **(c)** Confusion matrix

Figure 14. FSC under *biased split* on Dataset I . Training dynamics and final confusion matrix illustrate robustness to class imbalance.

models such as VGG19, EfficientNet, and ResNet. Despite their compact size, both architectures match or surpass these large models in accuracy while demonstrating strong robustness to distribution shifts. Their small parameter footprint and stability under perturbations highlight their suitability for deployment in edge or IoT environments.

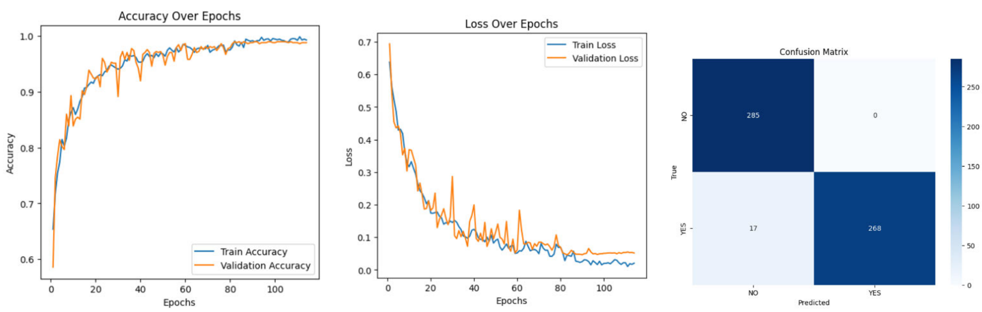

(a) accuracy over epochs **(b)** Loss over epochs **(c)** Confusion matrix

Figure 15. FSC evaluation under *added Gaussian noise* on Dataset I.

Computational efficiency and deployability. The FSC architecture is markedly compact, using only **0.216M** parameters (**0.83 MB**), about **70–600**$\times$ fewer than transfer learning models, such as MobileNetV2, ResNet50, EfficientNet, DenseNet121, VGG16 and VGG19. Despite this footprint, FSC attains exceptional accuracy on Dataset I, matching or exceeding transfer-learning baselines that span $\sim$14–143M parameters. Runtime measurements at a 224×224 resolution show a throughput of 52.76 FPS, which is comparable to DenseNet-121 (54.54 FPS) and meets real-time requirements. While MobileNetV2 and ResNet50 reach higher frame rates ($\approx$140 FPS), they incur $\geq$10–100$\times$ larger model sizes and memory budgets, such

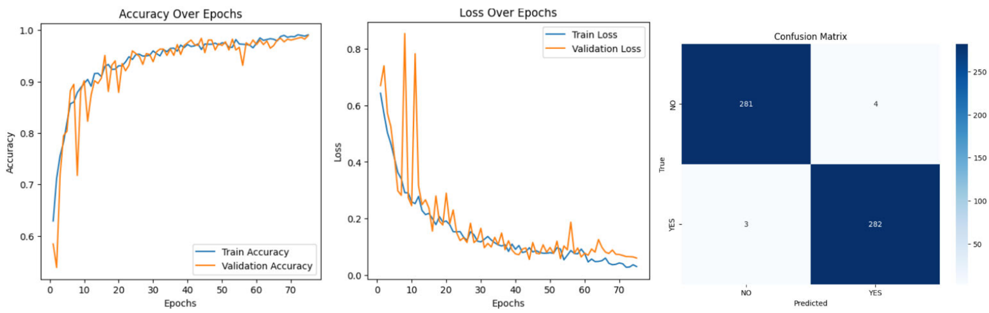

(a) accuracy over epochs **(b)** Loss over epochs **(c)** Confusion matrix

Figure 16. FSC evaluation under *Simulated Partial Occlusion* on Dataset I. Training and validation curves show stable convergence, and the confusion matrix reflects strong generalisation despite simulated Partial Occlusion injection, demonstrating robustness across resolutions.

as 8.49–89.68 MB vs. 0.83 MB for FSC. Overall, FSC offers a favourable accuracy–efficiency–latency trade-off, making it well-suited for *edge–cloud* deployments where on-device inference, low memory, and robust performance are required.

4.0.3 Publication III: Smart IoT-based Solutions for Neonatal Sleep Analysis

The findings reported in **Publication III** bring together the key advances in neonatal sleep analysis, highlighting the efficacy, robustness, and computational efficiency of the proposed methods. The experiments conducted across the datasets collected over four years, various channel setups, and different perturbation conditions consistently demonstrate that the combination of multiview feature extraction, AdaptiSelect feature selection, the STREAM module, and the rotational stacking classifier constitutes a robust and scalable framework for neonatal sleep staging.

10-Fold-CV: W_S vs. N_I vs. REM-II vs. Q_S: Across both 10-fold and LOSO cross-validation, the results consistently show that increasing the number of EEG channels improves classification performance, although the largest gain arises when moving from a single-channel to a dual-channel configuration. In a 10-fold CV, the model achieves an accuracy, F1, and Kappa of 0.8116, 0.8033, 0.7217 using one channel, improving to 0.8279, 0.8199, 0.7470 with two channels, and reaching 0.8774, 0.8735, 0.8214 with eight channels, respectively. Channel-pair analysis highlights that combinations involving F3, particularly **F3-T4**, provide the strongest dual-channel performance. The **LOSO-CV** for (W_S vs. N_I vs. REM-II vs. Q_S)) follows the same trend, with accuracies of 0.8047 (1-channel), 0.8165 (2-channel), and 0.8395 (8-channel), demonstrating the robustness of the approach under subject-independent evaluation. These results confirm that while eight channels yield the highest absolute performance, a two-channel configuration provides a strong accuracy–complexity trade-off that is well suited for clinically practical neonatal EEG systems.

10-fold CV: W_S vs. N_{II} vs. N_{III} vs. A_S: For the (W_S, N_{II}, N_{III}, A_S), the proposed methodology again shows a consistent performance gain as the number of EEG channels increases. In the 10-fold CV, accuracy/F1/Kappa improve from 0.7905/0.7737/-0.6988 (1 channel) to 0.8055/0.7956/0.7183 (2 channels), and further to 0.8656/-0.8589/0.8073 using all 8 channels. The **LOSO-CV** for (W_S vs. N_{II} vs. N_{III} vs. A_S), the results follow the same trend, with the eight-channel configuration achieving the highest metrics (accuracy 0.8274, F1 0.8167, Kappa 0.7473), outperforming both the dual-channel and single-channel settings. These results confirm that richer multichannel information substantially boosts classification performance, while the two-channel configuration still provides a competitive, lower-complexity alternative suitable for practical neonatal monitoring systems.

Impact of Three Different Noises on Model Performance: The robustness analysis demonstrates that neonatal EEG is highly sensitive to noise and motion artefacts, which can adversely affect classification performance when uncorrected. In our experiments, unfiltered motion artefacts reduced multichannel accuracy by 2.21 %, whereas applying the preprocessing pipeline (MSPCA and filtering) limited this reduction to only 0.44 %, confirming the effectiveness of the denoising strategy. Label purity also influenced performance: ensuring clean 30-second epochs improved accuracy by 1.3 % in 10-fold CV. Across the three noise types evaluated, Gaussian noise caused the largest degradation, with accuracy dropping by up to 3.21 % in the 8-channel configuration. Salt-and-pepper and dropout noise produced smaller reductions, remaining below 1.3 % across all channel setups. These findings confirm that incorporating robust preprocessing and feature selection steps (MSPCA and "AdaptiSelect") substantially stabilises model performance and enhances robustness under realistic neonatal EEG noise conditions.

Comparison with SOTA: A comparison with leading SOTA techniques for neonatal sleep staging demonstrates that the proposed method consistently achieves superior performance on all major evaluation metrics. Earlier CNN-based methods such as Conv-2D [113; 114] report relatively low accuracies (0.51–0.53), while feature-engineered or hybrid approaches including Stacking [115], BiLSTM [116], and MBCNN [117] achieve moderate improvements (0.66–0.71). Deep learning architectures adapted for neonatal data, such as DeepSleepNet [118] and MS-HNN [30], achieve accuracies around 0.72, with MS-HNN providing the strongest baseline (F1 = 0.73, $\kappa = 0.62$).

In Scenario S1, the proposed methodology achieves superior performance (Acc. = 0.81, F1 = 0.805, $\kappa = 0.72$), outperforming all SOTA benchmarks, including the best-performing MS-HNN model. In Scenario S2, the proposed method also exceeds the strongest existing deep learning models, achieving Acc. = 0.7745 and $\kappa = 0.6788$, compared with MS-HNN (Acc. = 0.702, $\kappa = 0.5992$) and DeepSleepNet (Acc. $\approx$ 0.70, $\kappa = 0.5802$). These consistent gains across scenarios underscore the robustness, generalisability, and discriminative strength of the proposed multiview feature and stacking-based framework for neonatal sleep staging.

Computational Complexity and Resource Requirements: The computational assessment shows that the stacking model remains lightweight and efficient across all channel configurations. Model size increases only modestly from 50.57 MB (1-channel) to 58.84 MB (8-channels), while inference time remains well within real-time limits (0.0979–0.1493 s). Peak memory usage scales with channel count, reaching 6004.95 KB for eight channels, with a corresponding rise in energy consumption (1.0481 J). For multiview feature extraction, DTCWT requires the highest memory (691 KB) and longest execution time (0.0397 s), whereas FAWT is the most efficient (0.0181 s). Feature fusion is computationally inexpensive (0.0050 s for one channel; 0.0401 s for eight channels), and STREAM processing adds negligible overhead. Together, these results indicate that the proposed pipeline is computationally viable for real-time neonatal sleep staging. The memory and timing requirements are compatible with edge devices (e.g., Raspberry Pi 3), supporting a future hybrid edge–cloud deployment for low-latency clinical monitoring.

4.0.4 Publication IV: Emotion Recognition with Minimal Wearable Sensing

Publication IV evaluates whether a single physiological signal (ECG) can reliably distinguish between positive and negative emotional states using a lightweight machine learning framework. Across all experiments, personalised models substantially outperform generalised ones. The best personalised ensemble model achieves an accuracy of 0.9559, compared with 0.6992 obtained by the top generalised model, underscoring the strong influence of inter-subject variability in physiological responses. An ablation study examines the role of different feature-selection strategies. While SelectKBest improves performance for several models, the hybrid method (ExtraTrees + SelectKBest) consistently produces the highest accuracies. In personalised settings, models such as ExtraTrees, Bagging, and Random Forest achieve accuracies in the range of 0.90–0.95 with hybrid feature selection, confirming their effectiveness in capturing subject-specific discriminatory features. In generalised settings, the hybrid method also yields the greatest improvements, with the ensemble model reaching 0.6992 and outperforming all baselines. These results collectively show that ECG alone provides a sufficiently rich signal for emotion classification when paired with appropriate feature engineering and personalised modelling. They also highlight the importance of hybrid feature selection in improving both robustness and interpretability. **Publication IV** supports the viability of minimal-sensing, low-complexity emotion-recognition systems suitable for wearable and resource-constrained environments.

Practical Significance for Real-World Deployment Beyond reporting relative reductions in model size and speed, the practical importance of computational efficiency should be assessed in the target deployment scenario. In Publications I and II, millisecond-level inference times and high throughput demonstrate that the proposed MRI models are fast enough for real-time or near-real-time decision support, while their substantially lower parameter counts enhance the feasibility of deployment on hardware with limited resources. In Publication III, acceptable performance must be evaluated alongside reduced sensing requirements, efficient data transmission, and robustness at the subject level, because neonatal sleep staging is designed for continuous monitoring rather than one-off predictions. In Publication IV, the usefulness of emotion recognition systems is determined not only by classification accuracy but also by their ability to operate reliably with short ECG segments and to incur low computational overhead in wearable applications. Thus, across all three domains, practical value hinges on striking an appropriate balance between accuracy, robustness, latency, and deployment feasibility.

5 Contribution of these Studies to the Overall Thesis Theme

This thesis aimed to investigate how computationally efficient AI methods can be designed for three clinically important, yet technically distinct, problems: brain tumour analysis from MRI, neonatal sleep staging from EEG, and emotion recognition from physiological signals. Although each publication focuses on its own dataset, modality, and task, together they form a coherent line of work on *lightweight, robust, and clinically aware* machine learning for health monitoring. In what follows, the main contributions of the four publications are summarised in relation to the overall thesis theme rather than repeating the full paper-specific result sections.

5.1 Alignment with the Overall Thesis Aims

Across all four studies, the thesis contributes to three overarching goals:

- designing resource-efficient AI models that remain feasible for edge or constrained clinical hardware, such as reduced model size, fast inference, minimal sensing;
- improving robustness and generalisability through subject-aware evaluation, such as LOSO validation, noise analysis, and principled feature selection;
- demonstrating that carefully engineered "classical" or hybrid approaches (optimised features + ensembles) can perform competitively with, or better than, heavier end-to-end deep networks in several health-related tasks.

The following sections provide a brief overview of each publication within this broader context.

5.2 Contribution of the Brain Tumour MRI Studies (Publications I–II)

The MRI-based studies address the first part of the thesis theme: efficient AI for brain tumour analysis.

- Both publications introduce and evaluate computationally lean CNN architectures, specifically FAC and FSC-based architectures, that operate on 2D MRI slices, reducing memory and computational demands while retaining high diagnostic performance.

- Through systematic perturbation experiments, such as adding noise, geometric and intensity variations, and monitoring of training dynamics (accuracy, loss, and confusion matrices across conditions), the studies quantify robustness and demonstrate how architectural choices, such as fuzzy atrous modules, improve stability under clinically realistic image degradations.

- Subject-level aggregation strategies and carefully designed cross-validation, for example, subject-stratified folds are used to reduce information leakage, providing a more realistic estimate of how models would behave in real deployments.

These contributions demonstrate that brain tumour classification can progress towards practical application without relying on excessively large, dense models, and they outline the design principles (efficiency, robustness, and subject-aware evaluation) that are subsequently applied in physiological signal research.

5.3 Contribution of the Neonatal Sleep Study (Publication III)

The neonatal sleep work extends the thesis from neuroimaging to EEG-based monitoring, while keeping a strong focus on computational efficiency and clinical practicality.

- A multiview feature fusion strategy is proposed, combining DTCWT, FAWT, ECOV, and spectral features into a rich representation of neonatal EEG. This is coupled with the proposed *AdaptiSelect* method, which reduces the dimensionality from thousands of raw features to a compact subset, such as from 2520 to 900 features for eight channels, and to 122 per single channel, while improving performance and stability.

- The work systematically analyses the trade-off between the number of EEG channels and classification accuracy. 10-fold, and LOSO-CV experiments show that two-channel configurations, such as F3 paired with temporal or central channels–T4, C3, or C4, achieve performance very close to that of eight-channel setups, while single-channel models remain clinically usable. This is central to the thesis theme of minimal, clinically feasible sensing.

- Robustness is explicitly studied by injecting Gaussian, salt-and-pepper, and dropout noise into the signals. The analysis shows that Gaussian noise has the most detrimental effect on the average performance drop across eight channels. In contrast, salt-and-pepper and dropout noise lead to smaller performance reductions. The denoising pipeline (bandpass filtering + MSPCA) reduces the impact of motion artefacts in ten-fold CV, and label purity analysis shows that cleaner epoch labelling can improve accuracy.

- Computational profiling demonstrates that feature extraction per epoch remains fast (e.g., FAWT ≈ 0.0181 s, DTCWT ≈ 0.0397 s), and that the stacking classifier has modest model size (up to ≈ 58.8 MB) and short inference times (≈ 0.10–0.15 s per test fold), supporting future edge-cloud deployment scenarios.

- Compared with SOTA neonatal sleep methods such as CNN- and BiLSTM-based models and multi-scale deep models, the proposed approach achieves higher four-stage classification performance, demonstrating that multiview features combined with ensembles can outperform several end-to-end deep learning baselines.

This research anchors the thesis in neonatal care, demonstrating how the same design ideas, multiview features, feature selection, channel reduction, robustness analysis, and computational profiling can be applied to transition from “research-grade” PSG to more scalable, NICU-friendly solutions.

5.4 Contribution of the Emotion Recognition Study (Publication IV)

The fourth publication completes the thesis by transitioning to emotion recognition from minimally sensed physiological signals, with a focus on ECG.

- It demonstrates that a single physiological modality (ECG) can be used to distinguish between positive and negative emotional states with high accuracy when combined with multidomain features and appropriate machine learning models. This aligns with the thesis goal of minimal sensing for real-time monitoring.

- An extensive comparison between generalised and personalised models shows a substantial performance gap of 0.2567, with personalised models outperforming their generalised counterparts. This highlights inter-subject variability as a key challenge and motivates the development of user-specific or adaptive models for affective computing.

- A hybrid feature selection pipeline is proposed and systematically evaluated in ablation studies. For generalised models, some classifiers, such as ensemble (Voting_Soft), benefit most from hybrid feature selection, while others favour KBest. For personalised models, hybrid feature selection consistently yields the best performance across top classifiers, confirming its role in improving accuracy without sacrificing computational efficiency.

- The analysis indicates that relatively simple, regularised methods, including KNN with distance weighting, ExtraTrees, random forest, and Multilayer Perceptron, can attain robust performance in a personalised context, supporting previous findings where ensembles with carefully designed features matched or surpassed deep learning models in physiological signal analysis.

5.5 Synthesis and Overall Impact

While the thesis presents four studies in different healthcare domains, they are unified by a consistent research theme: the development of computationally efficient AI methods for medical imaging and physiological signal analysis in resource-constrained settings. Across these studies, the work begins from practical and clinical constraints, including limited sensing channels, noisy data, heterogeneous subjects, and deployment limitations, and then develops methods that are explicitly efficient, robust, and deployable, rather than assuming that larger models and more data alone will solve these challenges. The novelty of this thesis lies not only in the individual methods proposed in each publication but also in demonstrating a unified design strategy for computationally efficient AI across heterogeneous healthcare tasks, including MRI-based brain-tumour classification, neonatal sleep-stage analysis from EEG, and ECG-based emotion recognition.

5.6 Shortcomings and Future Work

This thesis has several limitations, including the neonatal sleep EEG dataset originating from a single site, which restricts population diversity and external validity. Although the clinical scoring scheme contains five neonatal sleep stages, the present work focuses on a four-stage classification, and transitional or additional stages are not modelled. Moreover, a fixed 30 s epoch length is used throughout; the impact of shorter, longer, or multi-scale epoching on performance and real-time responsiveness remains unexplored.

For brain tumour MRI, the datasets were collected from multiple sites, but the tasks are restricted to binary classification (tumour vs. non-tumour), without addressing finer-grained grading or subtyping. This simplifies the clinical problem and may limit direct applicability in real-world neuro-oncology workflows, where tumour grading, subtype differentiation, and treatment-related changes are also important. Thus, the present study should be interpreted as a proof-of-concept showing that computationally efficient architectures can retain strong classification performance while substantially reducing model complexity. In addition, although the proposed method performed favourably compared with previous studies, formal statistical significance testing was not conducted. Therefore, small differences in performance metrics should be interpreted with caution, particularly regarding their clinical significance. Likewise, the ECG-based emotion analysis is limited to binary (positive vs. negative) affect and does not consider neutral or multi-class emotional states.

Pathways to clinical application Future work should further evaluate the proposed methods on larger and more diverse external datasets to improve robustness and clinical generalisability. For brain-tumour MRI (**Publication I and II**), an important next step is to move beyond binary classification towards tumour grading and subtype classification, which are more clinically challenging due to higher inter-class similarity and data imbalance. Although **Publication III** demonstrates strong potential for compact and IoT-compatible neonatal sleep staging, further work is needed before clinical use. A practical translation pathway would include external validation across independent, multicentre datasets, prospective testing in real neonatal monitoring environments, assessment of robustness to signal artefacts and device variability, and integration with neonatal care workflows. In addition, future studies should evaluate how such systems can support clinicians as decision-support tools rather than fully automated diagnostic systems. For ECG-based emotion recognition (**Publication IV**), extending the framework from binary affect classification to neutral and multi-class emotional states remains challenging due to stronger class overlap and greater inter-subject variability. In addition, exploring alternative epoch lengths, multi-scale temporal modelling, and validating the proposed methods on larger, more diverse cohorts will be important steps towards more robust, clinically generalisable AI solutions.

List of References

[1] Forrest N Iandola, Song Han, Matthew W Moskewicz, Khalid Ashraf, William J Dally, and Kurt Keutzer. Squeezenet: Alexnet-level accuracy with 50x fewer parameters and< 0.5 mb model size. *arXiv preprint arXiv:1602.07360*, 2016.

[2] Mark Sandler, Andrew Howard, Menglong Zhu, Andrey Zhmoginov, and Liang-Chieh Chen. Mobilenetv2: Inverted residuals and linear bottlenecks. In *Proceedings of the IEEE conference on computer vision and pattern recognition*, pages 4510–4520, 2018.

[3] Mingxing Tan and Quoc Le. Efficientnet: Rethinking model scaling for convolutional neural networks. In *International conference on machine learning*, pages 6105–6114. PMLR, 2019.

[4] Felix J Dorfner, Jay B Patel, Jayashree Kalpathy-Cramer, Elizabeth R Gerstner, and Christopher P Bridge. A review of deep learning for brain tumor analysis in mri. *NPJ Precision Oncology*, 9(1):2, 2025.

[5] Tarek Berghout. The neural frontier of future medical imaging: a review of deep learning for brain tumor detection. *Journal of Imaging*, 11(1):2, 2024.

[6] Amreen Batool and Yung-Cheol Byun. A lightweight multi-path convolutional neural network architecture using optimal features selection for multiclass classification of brain tumor using magnetic resonance images. *Results in Engineering*, 25:104327, 2025.

[7] Annisa Wulandari, Riyanto Sigit, and Mochamad Mobed Bachtiar. Brain tumor segmentation to calculate percentage tumor using mri. In *2018 International Electronics Symposium on Knowledge Creation and Intelligent Computing (IES-KCIC)*, pages 292–296. IEEE, 2018.

[8] Muhammad Irfan, Hafza Ayesha Siddiqa, Abdelwahed Nahliis, Chen Chen, Yan Xu, Laishuan Wang, Anum Nawaz, Abdulhamit Subasi, Tomi Westerlund, and Wei Chen. An ensemble voting approach with innovative multi-domain feature fusion for neonatal sleep stratification. *IEEE Access*, 12:206–218, 2024. doi: 10.1109/ACCESS.2023.3346059.

[9] Muhammad Irfan, Laishuan Wang, Husnain Shahid, Yan Xu, Abdulhamit Subasi, Adnan Munawar, Noman Mustafa, Chen Chen, Tomi Westurlund, and Wei Chen. Multidomain selective feature fusion and stacking based ensemble framework for eeg-based neonatal sleep stratification. *IEEE Journal of Biomedical and Health Informatics*, pages 1–10, 2025. doi: 10.1109/JBHI.2025.3530107.

[10] Duojiao Wu, Catherine M Rice, and Xiangdong Wang. Cancer bioinformatics: A new approach to systems clinical medicine. *BMC bioinformatics*, 13(1):1–4, 2012.

[11] Javier E Villanueva-Meyer, Marc C Mabray, and Soonmee Cha. Current clinical brain tumor imaging. *Neurosurgery*, 81(3):397–415, 2017.

[12] Ian Law, Nathalie L Albert, Javier Arbizu, Ronald Boellaard, Alexander Drzezga, Norbert Galldiks, Christian la Fougère, Karl-Josef Langen, Egesta Lopci, Val Lowe, et al. Joint eanm/eano/rano practice guidelines/snmmi procedure standards for imaging of gliomas using pet with radiolabelled amino acids and [18f] fdg: version 1.0. *European journal of nuclear medicine and molecular imaging*, 46(3):540–557, 2019.

[13] Sapna Singh Kshatri and Deepak Singh. Convolutional neural network in medical image analysis: a review. *Archives of Computational Methods in Engineering*, 30(4):2793–2810, 2023.

[14] Novsheena Rasool and Javaid Iqbal Bhat. Brain tumour detection using machine and deep learning: a systematic review. *Multimedia tools and applications*, 84(13):11551–11604, 2025.

[15] Surajit Das and Rajat Subhra Goswami. Advancements in brain tumor analysis: a comprehensive review of machine learning, hybrid deep learning, and transfer learning approaches for mri-based classification and segmentation. *Multimedia Tools and Applications*, 84(23):26645–26682, 2025.

[16] Sara Bouhafra and Hassan El Bahi. Deep learning approaches for brain tumor detection and classification using mri images (2020 to 2024): a systematic review. *Journal of Imaging Informatics in Medicine*, 38(3):1403–1433, 2025.

[17] Jyotismita Chaki and Marcin Woźniak. A deep learning based four-fold approach to classify brain mri: Btscnet. *Biomedical Signal Processing and Control*, 85:104902, 2023.

[18] Santhos A. Kumar, Anil Kumar, Varun Bajaj, and Girish Kumar Singh. An improved fuzzy min–max neural network for data classification. *IEEE Transactions on Fuzzy Systems*, 28(9):1910–1924, 2020. doi: 10.1109/TFUZZ.2019.2924396.

[19] Muhammad Irfan, Abdulhamit Subasi, Hassan Mehdi, Tomi Westerlund, and Wei Chen. Fuzzy-based atrous convolution for brain tumor detection using mri. In *2024 IEEE International Conference on Progress in Informatics and Computing (PIC)*, pages 280–289. IEEE, 2024.

[20] Muhammad Irfan, Anum Nawaz, Riku Klén, Abdulhamit Subasi, Tomi Westerlund, and Wei Chen. Improved brain tumor detection in mri: Fuzzy sigmoid convolution in deep learning. In *2025 International Joint Conference on Neural Networks (IJCNN)*, pages 1–8, 2025. doi: 10.1109/IJCNN64981.2025.11227858.

[21] Mohsen Asghari Ilani and Yaser M Banad. Brain tumor detection through diverse cnn architectures in iot healthcare industries: Fast r-cnn, u-net, transfer learning-based cnn, and fully connected cnn. *arXiv preprint arXiv:2509.05821*, 2025.

[22] Ishak Pacal, Omer Celik, Bilal Bayram, and Antonio Cunha. Enhancing efficientnetv2 with global and efficient channel attention mechanisms for accurate mri-based brain tumor classification. *Cluster Computing*, 27(8):11187–11212, 2024.

[23] International Data Corporation. Worldwide quarterly wearable device tracker. `https://www.idc.com/promo/wearablevendor/`, 2025. Accessed: 2025-09-09.

[24] AARP. Aarp research insights on technology. `https://www.aarp.org/pri/topics/technology/internet-media-devices/aarp-research-insights-technology/`, 2025. Published: July 3, 2025. Accessed: September 9, 2025.

[25] World Health Organization. Levels and trends in child mortality report 2021. World Health Organization, 2021. URL `https://www.who.int/news-room/fact-sheets/detail/levels-and-trends-in-child-mortality-report-2021`. Accessed: 15 March 2024.

[26] World Health Organization. Newborn mortality, report march 2024. World Health Organization, 2024. URL `https://www.who.int/news-room/fact-sheets/detail/newborn-mortality#:~:text=The%20world%20has%20made%20substantial,%2Dneonatal%20under%2D5%20mortality`. Accessed: 25 March 2024.

[27] Kritiprasanna Das, Vivek Kumar Singh, and Ram Bilas Pachori. Introduction to eeg signal recording and processing. In *Artificial Intelligence Enabled Signal Processing based Models for Neural Information Processing*, pages 1–19. CRC Press, 2024.

[28] Dale Purves, George J Augustine, David Fitzpatrick, Lawrence C Katz, Anthony-Samuel LaMantia, James O McNamara, and S Mark Williams. Neuroglial cells. *Neuroscience*, 2001.

[29] Jeffrey W Britton, Lauren C Frey, Jennifer L Hopp, Pearce Korb, Mohamad Z Koubeissi, William E Lievens, Elia M Pestana-Knight, and Erk K St Louis. Electroencephalography (eeg): An introductory text and atlas of normal and abnormal findings in adults, children, and infants. 2016.

[30] Hangyu Zhu, Laishuan Wang, Ning Shen, Yonglin Wu, Shu Feng, Yan Xu, Chen Chen, and Wei Chen. Ms-hnn: Multi-scale hierarchical neural network with squeeze and excitation block for neonatal sleep staging using a single-channel eeg. *IEEE Transactions on Neural Systems and Rehabilitation Engineering*, 31:2195–2204, 2023. doi: 10.1109/TNSRE.2023.3266876.

[31] Britta Hüning, Tobias Storbeck, Nora Bruns, Frauke Dransfeld, Julia Hobrecht, Julia Karpienski, Selma Sirin, Bernd Schweiger, Christel Weiss, Ursula Felderhoff-Müser, et al. Relationship between brain function (aeeg) and brain structure (mri) and their predictive value for neurodevelopmental outcome of preterm infants. *European journal of pediatrics*, 177:1181–1189, 2018.

[32] Renée A Shellhaas, Taeun Chang, Tammy Tsuchida, Mark S Scher, James J Riviello, Nicholas S Abend, Sylvie Nguyen, Courtney J Wusthoff, and Robert R Clancy. The american clinical neurophysiology society's guideline on continuous electroencephalography monitoring in neonates. *Journal of clinical neurophysiology*, 28(6):611–617, 2011.

[33] Linda GM van Rooij, Linda S de Vries, Alexander C van Huffelen, and Mona C Toet. Additional value of two-channel amplitude integrated eeg recording in full-term infants with unilateral brain injury. *Archives of Disease in Childhood-Fetal and Neonatal Edition*, 95(3):F160–F168, 2010.

[34] Jayant N Acharya and Vinita J Acharya. Overview of eeg montages and principles of localization. *Journal of Clinical Neurophysiology*, 36(5):325–329, 2019.

[35] Alfred L Loomis, E Newton Harvey, and Garret A Hobart. Cerebral states during sleep, as studied by human brain potentials. *Journal of experimental psychology*, 21(2):127, 1937.

[36] Pierre Gloor. Hans berger on electroencephalography. *American Journal of EEG Technology*, 9 (1):1–8, 1969.

[37] Mohamed El-Dib, Taeun Chang, Tammy N Tsuchida, and Robert R Clancy. Amplitude-integrated electroencephalography in neonates. *Pediatric neurology*, 41(5):315–326, 2009.

[38] Andreea M Pavel, Janet M Rennie, Linda S de Vries, Mats Blennow, Adrienne Foran, Divyen K Shah, Ronit M Pressler, Olga Kapellou, Eugene M Dempsey, Sean R Mathieson, et al. A machine-learning algorithm for neonatal seizure recognition: a multicentre, randomised, controlled trial. *The Lancet Child & Adolescent Health*, 4(10):740–749, 2020.

[39] Faye S Silverstein, Frances E Jensen, Terrie Inder, Lena Hellstrom-Westas, Deborah Hirtz, and Donna M Ferriero. Improving the treatment of neonatal seizures: National institute of neurological disorders and stroke workshop report. *The Journal of pediatrics*, 153(1):12–15, 2008.

[40] Hafza Ayesha Siddiqa, Zhenning Tang, Yan Xu, Laishuan Wang, Muhammad Irfan, Saadullah Farooq Abbasi, Anum Nawaz, Chen Chen, and Wei Chen. Single-channel eeg data analysis using a multi-branch cnn for neonatal sleep staging. *IEEE Access*, 12:29910–29925, 2024. doi: 10.1109/ACCESS.2024.3365570.

[41] GB Boylan, L Burgoyne, C Moore, B O'flaherty, and JM Rennie. An international survey of eeg use in the neonatal intensive care unit. *Acta paediatrica*, 99(8):1150–1155, 2010.

[42] Robertino Dilena, Federico Raviglione, Gaetano Cantalupo, Duccio M Cordelli, Paola De Liso, Matteo Di Capua, Raffaele Falsaperla, Fabrizio Ferrari, Monica Fumagalli, Silvia Lori, et al. Consensus protocol for eeg and amplitude-integrated eeg assessment and monitoring in neonates. *Clinical Neurophysiology*, 132(4):886–903, 2021.

[43] V. Gerla, K. Paul, L. Lhotska, and V. Krajca. Multivariate analysis of full-term neonatal polysomnographic data. *IEEE Transactions on Information Technology in Biomedicine*, 13(1): 104–110, 2009. doi: 10.1109/TITB.2008.2007193.

[44] Nicholas S Abend, Ram Mani, Tammy N Tschuda, Tae Chang, Alexis A Topjian, Maureen Donnelly, Denise LaFalce, Margaret C Krauss, Sarah E Schmitt, and Joshua M Levine. Eeg monitoring during therapeutic hypothermia in neonates, children, and adults. *American journal of electroneurodiagnostic technology*, 51(3):141–164, 2011.

[45] Maarten De Vos, Wouter Deburchgraeve, PJ Cherian, Vladimir Matic, RM Swarte, Paul Govaert, Gerhard Henk Visser, and Sabine Van Huffel. Automated artifact removal as preprocessing refines neonatal seizure detection. *Clinical Neurophysiology*, 122(12):2345–2354, 2011.

[46] De Maarten Vos, Stephanie Riès, Katrien Vanderperren, Bart Vanrumste, Francois-Xavier Alario, Van Sabine Huffel, and Boris Burle. Removal of muscle artifacts from eeg recordings of spoken language production. *Neuroinformatics*, 8:135–150, 2010.

[47] Vitaly Schetinin and Joachim Schult. The combined technique for detection of artifacts in clinical electroencephalograms of sleeping newborns. *IEEE Transactions on Information Technology in Biomedicine*, 8(1):28–35, 2004.

[48] Mona C Toet and Petra MA Lemmers. Brain monitoring in neonates. *Early human development*, 85(2):77–84, 2009.

[49] Lachlan Webb, Minna Kauppila, James A Roberts, Sampsa Vanhatalo, and Nathan J Stevenson. Automated detection of artefacts in neonatal eeg with residual neural networks. *Computer Methods and Programs in Biomedicine*, 208:106194, 2021.

[50] M. Kauppila, S. Vanhatalo, and N.J. Stevenson. Artifact detection in neonatal eeg using gaussian mixture models. In *EMBEC & NBC 2017: Joint Conference of the European Medical and Biological Engineering Conference (EMBEC) and the Nordic-Baltic Conference on Biomedical Engineering and Medical Physics (NBC), Tampere, Finland, June 2017*, pages 221–224. Springer Singapore, 2018.

[51] Nathan J Stevenson, John M O'Toole, Irina Korotchikova, and Geraldine B Boylan. Artefact detection in neonatal eeg. In *2014 36th Annual International Conference of the IEEE Engineering in Medicine and Biology Society*, pages 926–929. IEEE, 2014.

[52] Vladimir Matic, Perumpillichira J Cherian, Ninah Koolen, Gunnar Naulaers, Renate M Swarte, Paul Govaert, Sabine Van Huffel, and Maarten De Vos. Holistic approach for automated background eeg assessment in asphyxiated full-term infants. *Journal of neural engineering*, 11(6): 066007, 2014.

[53] Saeed Montazeri Moghadam, Elana Pinchefsky, Ilse Tse, Viviana Marchi, Jukka Kohonen, Minna Kauppila, Manu Airaksinen, Karoliina Tapani, Päivi Nevalainen, Cecil Hahn, et al. Building an open source classifier for the neonatal eeg background. 2021.

[54] Pierre Bourgoin, Victoire Barrault, Gauthier Loron, Alexandre Roger, Emmanuelle Bataille, Laurène Leclair-Visonneau, Nicolas Joram, and Alexis Chenouard. Interrater agreement between critical care providers for background classification and seizure detection after implementation of amplitude-integrated electroencephalography in neonates, infants, and children. *Journal of Clinical Neurophysiology*, 37(3):259–262, 2020.

[55] Nathan J Stevenson, Maria-Luisa Tataranno, Anna Kaminska, Elena Pavlidis, Robert R Clancy, Elke Griesmaier, James A Roberts, Katrin Klebermass-Schrehof, and Sampsa Vanhatalo. Reliability and accuracy of eeg interpretation for estimating age in preterm infants. *Annals of Clinical and Translational Neurology*, 7(9):1564–1573, 2020.

[56] Hangyu Zhu, Yao Guo, Yonglin Wu, Yiyuan Zhang, Ning Shen, Yan Xu, Laishuan Wang, Chen Chen, and Wei Chen. Magsleepnet: Adaptively multi-scale temporal focused sleep staging model for multi-age groups. *Expert Systems with Applications*, 240:122549, 2024.

[57] Saeed Montazeri Moghadam. Advancing automated eeg analysis for neonatal intensive care: From engineering to bedside solutions. 2023.

[58] Joseph L Fleiss, Bruce Levin, and Myunghee Cho Paik. *Statistical methods for rates and proportions*. john wiley & sons, 2013.

[59] Giuseppe Buonocore and Rodolfo Bracci Michael Weindling. neonatology a practical approach to neonatal diseases. Springer, 2012.

[60] Mark S Scher, Mingui Sun, Doris A Steppe, Robert D Guthrie, and Robert J Sclabassi. Comparisons of eeg spectral and correlation measures between healthy term and preterm infants. *Pediatric neurology*, 10(2):104–108, 1994.

[61] Joseph J Volpe. Neurology of the newborn e-book. 2008.

[62] Monique André, M-D Lamblin, Anne-Marie d'Allest, Lilia Curzi-Dascalova, FTSNT Moussalli-Salefranque, S Nguyen The Tich, M-F Vecchierini-Blineau, Fabrice Wallois, E Walls-Esquivel, and P Plouin. Electroencephalography in premature and full-term infants. developmental features and glossary. *Neurophysiologie clinique/Clinical neurophysiology*, 40(2):59–124, 2010.

[63] Danièle Jouvet-Mounier, Liliane Astic, and Daniel Lacote. Ontogenesis of the states of sleep in rat, cat, and guinea pig during the first postnatal month. *Developmental Psychobiology: The Journal of the International Society for Developmental Psychobiology*, 2(4):216–239, 1969.

[64] Gerald A Marks, James P Shaffery, Arie Oksenberg, Samuel G Speciale, and Howard P Roffwarg. A functional role for rem sleep in brain maturation. *Behavioural brain research*, 69(1-2): 1–11, 1995.

[65] Patricio Peirano, Cecilia Algarín, and Ricardo Uauy. Sleep-wake states and their regulatory mechanisms throughout early human development. *The Journal of pediatrics*, 143(4):70–79, 2003.

[66] William P Fifer, Dana L Byrd, Michelle Kaku, Inge-Marie Eigsti, Joseph R Isler, Jillian Grose-Fifer, Amanda R Tarullo, and Peter D Balsam. Newborn infants learn during sleep. *Proceedings of the National Academy of Sciences*, 107(22):10320–10323, 2010.

[67] Elizabeth Hennevin, Bernard Hars, Catherine Maho, and Vincent Bloch. Processing of learned information in paradoxical sleep: relevance for memory. *Behavioural brain research*, 69(1-2): 125–135, 1995.

[68] Catherine Maho and Vincent Bloch. Responses of hippocampal cells can be conditioned during paradoxical sleep. *Brain research*, 581(1):115–122, 1992.

[69] H Denenberg Victor and B Thoman Evelyn. Evidence for a functional role for active (rem) sleep in infancy. *Sleep*, 4(2):185–191, 1981.

[70] Jeffrey W Britton, Lauren C Frey, Jennifer L Hopp, Pearce Korb, Mohamad Z Koubeissi, William E Lievens, Elia M Pestana-Knight, and Erk K St Louis. Electroencephalography (eeg): An introductory text and atlas of normal and abnormal findings in adults, children, and infants. 2016.

[71] Madeleine M Grigg-Damberger. The visual scoring of sleep in infants 0 to 2 months of age. *Journal of clinical sleep medicine*, 12(3):429–445, 2016.

[72] Lilia Curzi-Dascalova, Patricio Peirano, and Françoise Morel-Kahn. Development of sleep states in normal premature and full-term newborns. *Developmental Psychobiology: The Journal of the International Society for Developmental Psychobiology*, 21(5):431–444, 1988.

[73] Saadullah Farooq Abbasi, Awais Abbas, Iftikhar Ahmad, Mohammed S Alshehri, Sultan Almakdi, Yazeed Yasin Ghadi, and Jawad Ahmad. Automatic neonatal sleep stage classification: A comparative study. *Heliyon*, 2023.

[74] Awais Abbas, Hafiz Sheraz Sheikh, Haris Ahmad, and Saadullah Farooq Abbasi. An iot and machine learning-based neonatal sleep stage classification. *Manuscript on ResearchGate. https://www. researchgate. net/publication/369761857_ An_IoT_and_Machine_Learning-based_Neonatal_Sleep_Stage_Classification (accessed on 08/05/2023).*

[75] Saeed Montazeri Moghadam, Päivi Nevalainen, Nathan J Stevenson, and Sampsa Vanhatalo. Sleep state trend (sst), a bedside measure of neonatal sleep state fluctuations based on single eeg channels. *Clinical Neurophysiology*, 143:75–83, 2022.

[76] Amir H Ansari, Ofelie De Wel, Kirubin Pillay, Anneleen Dereymaeker, Katrien Jansen, Sabine Van Huffel, Gunnar Naulaers, and Maarten De Vos. A convolutional neural network outperforming state-of-the-art sleep staging algorithms for both preterm and term infants. 17(1): 016028, 2020. doi: 10.1088/1741-2552/ab5469. URL `https://dx.doi.org/10.1088/1741-2552/ab5469`.

[77] Saadullah Farooq Abbasi, Jawad Ahmad, Ahsen Tahir, Muhammad Awais, Chen Chen, Muhammad Irfan, Hafiza Ayesha Siddiqa, Abu Bakar Waqas, Xi Long, Bin Yin, et al. Eeg-based neonatal sleep-wake classification using multilayer perceptron neural network. *IEEE Access*, 8:183025–183034, 2020.

[78] Yue Wu, Jiaming Liu, Maoguo Gong, Zhixiao Liu, Qiguang Miao, and Wenping Ma. Mpct: Multiscale point cloud transformer with a residual network. *IEEE Transactions on Multimedia*, 26:3505–3516, 2024. doi: 10.1109/TMM.2023.3312855.

[79] Yongzhe Yuan, Yue Wu, Xiaolong Fan, Maoguo Gong, Wenping Ma, and Qiguang Miao. Egst: Enhanced geometric structure transformer for point cloud registration. *IEEE Transactions on Visualization and Computer Graphics*, 30(9):6222–6234, 2024. doi: 10.1109/TVCG.2023.3329578.

[80] Muhammad Irfan, Husnain Jawad, Barkoum Betra Felix, Saadullah Farooq Abbasi, Anum Nawaz, Saeed Akbarzadeh, Muhammad Awais, Lin Chen, Tomi Westerlund, and Wei Chen. Non-wearable iot-based smart ambient behavior observation system. *IEEE Sensors Journal*, 21 (18):20857–20869, 2021. doi: 10.1109/JSEN.2021.3097392.

[81] Muhammad Irfan, Laishuan Wang, Husnain Shahid, Yan Xu, Abdulhamit Subasi, Adnan Munawar, Noman Mustafa, Chen Chen, Tomi Westurlund, and Wei Chen. Multidomain selective feature fusion and stacking based ensemble framework for eeg-based neonatal sleep stratification. *IEEE Journal of Biomedical and Health Informatics*, 2025.

[82] I Dewa Gede Hari Wisana Triwiyanto and Bedjo Utomo Sumber. Oxigen concentration detector in the continuous positive airway pressure for sleep apnea therapy based on iot technology. In *2021 International Seminar on Application for Technology of Information and Communication (iSemantic)*, pages 156–160, 2021. doi: 10.1109/iSemantic52711.2021.9573207.

[83] Elizabeth A Kensinger. Remembering emotional experiences: The contribution of valence and arousal. *Reviews in the Neurosciences*, 15(4):241–252, 2004.

[84] Ed Diener, Stuti Thapa, and Louis Tay. Positive emotions at work. *Annual review of organizational psychology and organizational behavior*, 7(1):451–477, 2020.

[85] Evgenia Gkintoni, Anthimos Aroutzidis, Hera Antonopoulou, and Constantinos Halkiopoulos. From neural networks to emotional networks: A systematic review of eeg-based emotion recognition in cognitive neuroscience and real-world applications. *Brain Sciences*, 15(3):220, 2025.

[86] Shiqing Zhang, Yijiao Yang, Chen Chen, Xingnan Zhang, Qingming Leng, and Xiaoming Zhao. Deep learning-based multimodal emotion recognition from audio, visual, and text modalities: A systematic review of recent advancements and future prospects. *Expert Systems with Applications*, 237:121692, 2024.

[87] Huan Liu, Tianyu Lou, Yuzhe Zhang, Yixiao Wu, Yang Xiao, Christian S Jensen, and Dalin Zhang. Eeg-based multimodal emotion recognition: A machine learning perspective. *IEEE Transactions on Instrumentation and Measurement*, 2024.

[88] Runfang Guo, Hongfei Guo, Liwen Wang, Mengmeng Chen, Dong Yang, and Bin Li. Development and application of emotion recognition technology—a systematic literature review. *BMC psychology*, 12(1):95, 2024.

[89] Maja Pantic, George Caridakis, Elisabeth André, Jonghwa Kim, Kostas Karpouzis, and Stefanos Kollias. Multimodal emotion recognition from low-level cues. In *Emotion-oriented systems: The humaine handbook*, pages 115–132. Springer, 2010.

[90] Loic Kessous, Ginevra Castellano, and George Caridakis. Multimodal emotion recognition in speech-based interaction using facial expression, body gesture and acoustic analysis. *Journal on Multimodal User Interfaces*, 3:33–48, 2010.

[91] Sidney K D'mello and Jacqueline Kory. A review and meta-analysis of multimodal affect detection systems. *ACM computing surveys (CSUR)*, 47(3):1–36, 2015.

[92] Moataz El Ayadi, Mohamed S Kamel, and Fakhri Karray. Survey on speech emotion recognition: Features, classification schemes, and databases. *Pattern recognition*, 44(3):572–587, 2011.

[93] Daniel Canedo and António JR Neves. Facial expression recognition using computer vision: A systematic review. *Applied Sciences*, 9(21):4678, 2019.

[94] Gloria Cosoli, Angelica Poli, Lorenzo Scalise, and Susanna Spinsante. Heart rate variability analysis with wearable devices: Influence of artifact correction method on classification accuracy for emotion recognition. In *2021 IEEE International Instrumentation and Measurement Technology Conference (I2MTC)*, pages 1–6, 2021. doi: 10.1109/I2MTC50364.2021.9459828.

[95] Yixiang Dai, Xue Wang, Xuanping Li, and Pengbo Zhang. Reputation-driven multimodal emotion recognition in wearable biosensor network. In *2015 IEEE International Instrumentation and Measurement Technology Conference (I2MTC) Proceedings*, pages 1747–1752, 2015. doi: 10.1109/I2MTC.2015.7151544.

[96] Guanglong Du, Qinglin Tan, Chunquan Li, Xueqian Wang, Shaohua Teng, and Peter X. Liu. A noncontact emotion recognition method based on complexion and heart rate. *IEEE Transactions on Instrumentation and Measurement*, 71:1–14, 2022. doi: 10.1109/TIM.2022.3194858.

[97] Yueyang Li, Weiming Zeng, Wenhao Dong, Di Han, Lei Chen, Hongyu Chen, Zijian Kang, Shengyu Gong, Hongjie Yan, Wai Ting Siok, and Nizhuan Wang. A tale of single-channel electroencephalography: Devices, datasets, signal processing, applications, and future di-

rections. *IEEE Transactions on Instrumentation and Measurement*, 74:1–20, 2025. doi: 10.1109/TIM.2025.3556900.

[98] Yun-Kai Li, Qing-Hao Meng, Tian-Hao Yang, Ya-Xin Wang, and Hui-Rang Hou. Touch gesture and emotion recognition using decomposed spatiotemporal convolutions. *IEEE Transactions on Instrumentation and Measurement*, 71:1–9, 2022. doi: 10.1109/TIM.2022.3147338.

[99] Andrea Apicella, Pasquale Arpaia, Francesco Isgrò, Giovanna Mastrati, and Nicola Moccaldi. A survey on eeg-based solutions for emotion recognition with a low number of channels. *IEEE Access*, 10:117411–117428, 2022. doi: 10.1109/ACCESS.2022.3219844.

[100] Karim Alghoul, Hussein Al Osman, and Abdulmotaleb El Saddik. Enhancing generalization in ppg-based emotion measurement with a cnn-tcn-lstm model. In *2025 IEEE International Instrumentation and Measurement Technology Conference (I2MTC)*, pages 1–6, 2025. doi: 10.1109/I2MTC62753.2025.11079085.

[101] Marco Schlosser, Harriet Demnitz-King, Tim Whitfield, Miranka Wirth, and Natalie L Marchant. Repetitive negative thinking is associated with subjective cognitive decline in older adults: a cross-sectional study. *BMC psychiatry*, 20:1–10, 2020.

[102] Rajal Devshi, Sarah Shaw, Jordan Elliott-King, Eef Hogervorst, Avinash Hiremath, Latha Velayudhan, Satheesh Kumar, Sarah Baillon, and Stephan Bandelow. Prevalence of behavioural and psychological symptoms of dementia in individuals with learning disabilities. *Diagnostics*, 5(4):564–576, 2015.

[103] Xudong Yang, Hongli Yan, Anguo Zhang, Pan Xu, Sio Hang Pan, Mang I Vai, and Yueming Gao. Emotion recognition based on multimodal physiological signals using spiking feed-forward neural networks. *Biomedical Signal Processing and Control*, 91:105921, 2024.

[104] Caroline Cobb (Amey). Emotions, aggression, and stress. `https://pressbooks.library.vcu.edu/psyc629/chapter/emotions-aggression-stress/`, 2024. Accessed: 2025-05-23.

[105] Polar Electro Oy. Polar BLE SDK. `https://github.com/polarofficial/polar-ble-sdk`, 2025. Accessed: 2025-05-23.

[106] Muhammad Irfan, Laishuan Wang, Yan Xu, Abdulhamit Subasi, Chen Chen, Riku Klen, Tomi Westurlund, and Wei Chen. Smart iot-based solutions for neonatal sleep stratification: Single-dual channel eeg, adaptiselect, multview fusion, & rotational ensemble stacking. *IEEE Internet of Things Journal*, 2025.

[107] Abhranta Panigrahi. Brain tumor detection mri. `https://www.kaggle.com/datasets/abhranta/brain-tumor-detection-mri`, 2021. Accessed: December 14, 2024.

[108] Maciej A Mazurowski, Kal Clark, Nicholas M Czarnek, Parisa Shamsesfandabadi, Katherine B Peters, and Ashirbani Saha. Radiogenomics of lower-grade glioma: algorithmically-assessed tumor shape is associated with tumor genomic subtypes and patient outcomes in a multi-institutional study with the cancer genome atlas data. *Journal of neuro-oncology*, 133:27–35, 2017.

[109] Maciej Behnke, Mikołaj Buchwald, Adam Bykowski, Szymon Kupiński, and Lukasz D Kaczmarek. Psychophysiology of positive and negative emotions, dataset of 1157 cases and 8 biosignals. *Scientific Data*, 9(1):10, 2022.

[110] Amitava Halder and Debangshu Dey. Atrous convolution aided integrated framework for lung nodule segmentation and classification. *Biomedical Signal Processing and Control*, 82: 104527, 2023.

[111] Rangan Das, Samayan Bhattacharya, Swadesh Jana, Ujjwal Maulik, and Sanghamitra Bandyopadhyay. Improving lung ct analysis through fuzzy dilated convolution attention. In *2023 IEEE 3rd Applied Signal Processing Conference (ASPCON)*, pages 71–76, 2023. doi: 10.1109/ASPCON59071.2023.10396336.

[112] Muhammad Irfan, Peng Shun, Barkoum Betra Felix, Noman Mustafa, Saadullah Farooq Abbasi, Abdelwahed Nahli, Abdulhamit Subasi, Tomi Westerlund, and Wei Chen. An iot-based non-contact ecg system: Sole of the feet/hands palm. *IEEE Internet of Things Journal*, 2023.

[113] Amir Hossein Ansari, Ofelie De Wel, Mario Lavanga, Alexander Caicedo, Anneleen Dereymaeker, Katrien Jansen, Jan Vervisch, Maarten De Vos, Gunnar Naulaers, and Sabine Van Huffel. Quiet sleep detection in preterm infants using deep convolutional neural networks. *Journal of neural engineering*, 15(6):066006, 2018.

[114] Amir H Ansari, Ofelie De Wel, Kirubin Pillay, Anneleen Dereymaeker, Katrien Jansen, Sabine Van Huffel, Gunnar Naulaers, and Maarten De Vos. A convolutional neural network outperforming state-of-the-art sleep staging algorithms for both preterm and term infants. *Journal of Neural Engineering*, 17(1):016028, 2020.

[115] Saadullah Farooq Abbasi, Harun Jamil, and Wei Chen. Eeg-based neonatal sleep stage classification using ensemble learning. *Comput. Mater. Contin*, 70:4619–4633, 2022.

[116] Hojat Ghimatgar, Kamran Kazemi, Mohammad Sadegh Helfroush, Kirubin Pillay, Anneleen Dereymaker, Katrien Jansen, Maarten De Vos, and Ardalan Aarabi. Neonatal eeg sleep stage classification based on deep learning and hmm. *Journal of neural engineering*, 17(3):036031, 2020.

[117] Hafza Ayesha Siddiqa, Zhenning Tang, Yan Xu, Laishuan Wang, Muhammad Irfan, Saadullah Farooq Abbasi, Anum Nawaz, Chen Chen, and Wei Chen. Single-channel eeg data analysis using a multi-branch cnn for neonatal sleep staging. *IEEE Access*, 2024.

[118] Akara Supratak, Hao Dong, Chao Wu, and Yike Guo. Deepsleepnet: A model for automatic sleep stage scoring based on raw single-channel eeg. *IEEE Transactions on Neural Systems and Rehabilitation Engineering*, 25(11):1998–2008, 2017.

TURUN
YLIOPISTO
UNIVERSITY
OF TURKU

Painosalama, Turku, Finland 2026

ISBN 978-952-02-0652-9 (PRINT)
ISBN 978-952-02-0653-6 (PDF)
ISSN 2736-9390 (Painettu/Print)
ISSN 2736-9684 (Sähköinen/Online)